

A SUSY $SU(5) \times T'$ Unified Model of Flavour with large θ_{13}

Aurora Meroni^{a, 1}, S. T. Petcov^{a,b, 2}, Martin Spinrath^{a, 3},

^a *SISSA/ISAS and INFN,
Via Bonomea 265, I-34136 Trieste, Italy*

^b *Kavli IPMU, University of Tokyo, Tokyo, Japan*

Abstract

We present a SUSY $SU(5) \times T'$ unified flavour model with type I see-saw mechanism of neutrino mass generation, which predicts the reactor neutrino angle to be $\theta_{13} \approx 0.14$ close to the recent results from the Daya Bay and RENO experiments. The model predicts also values of the solar and atmospheric neutrino mixing angles, which are compatible with the existing data. The T' breaking leads to tri-bimaximal mixing in the neutrino sector, which is perturbed by sizeable corrections from the charged lepton sector. The model exhibits geometrical CP violation, where all complex phases have their origin from the complex Clebsch–Gordan coefficients of T' . The values of the Dirac and Majorana CP violating phases are predicted. For the Dirac phase in the standard parametrisation of the neutrino mixing matrix we get a value close to 90° : $\delta \cong \pi/2 - 0.45\theta^c \cong 84.3^\circ$, θ^c being the Cabibbo angle. The neutrino mass spectrum can be with normal ordering (2 cases) or inverted ordering. In each case the values of the three light neutrino masses are predicted with relatively small uncertainties, which allows to get also unambiguous predictions for the $(\beta\beta)_{0\nu}$ -decay effective Majorana mass.

¹E-mail: aurora.meroni@sissa.it

²Also at: Institute of Nuclear Research and Nuclear Energy, Bulgarian Academy of Sciences, 1784 Sofia, Bulgaria.

³E-mail: spinrath@sissa.it

1 Introduction

Understanding the origin of the patterns of neutrino masses and mixing, emerging from the neutrino oscillation, ${}^3\text{H}$ β -decay, etc. data is one of the most challenging problems in neutrino physics. It is part of the more general fundamental problem in particle physics of understanding the origins of flavour, i.e., of the patterns of the quark, charged lepton and neutrino masses and of the quark and lepton mixing.

At present we have compelling evidence for existence of mixing of three light massive neutrinos ν_i , $i = 1, 2, 3$, in the weak charged lepton current (see, e.g., [1]). The masses m_i of the three light neutrinos ν_i do not exceed approximately 1 eV, $m_i \lesssim 1$ eV, i.e., they are much smaller than the masses of the charged leptons and quarks. The three light neutrino mixing is described (to a good approximation) by the Pontecorvo, Maki, Nakagawa, Sakata (PMNS) 3×3 unitary mixing matrix, U_{PMNS} . In the widely used standard parametrisation [1], U_{PMNS} is expressed in terms of the solar, atmospheric and reactor neutrino mixing angles θ_{12} , θ_{23} and θ_{13} , respectively, and one Dirac - δ , and two Majorana [2] - α_{21} and α_{31} , CP violating phases:

$$U_{\text{PMNS}} \equiv U = V(\theta_{12}, \theta_{23}, \theta_{13}, \delta) Q(\alpha_{21}, \alpha_{31}), \quad (1.1)$$

where

$$V = \begin{pmatrix} 1 & 0 & 0 \\ 0 & c_{23} & s_{23} \\ 0 & -s_{23} & c_{23} \end{pmatrix} \begin{pmatrix} c_{13} & 0 & s_{13}e^{-i\delta} \\ 0 & 1 & 0 \\ -s_{13}e^{i\delta} & 0 & c_{13} \end{pmatrix} \begin{pmatrix} c_{12} & s_{12} & 0 \\ -s_{12} & c_{12} & 0 \\ 0 & 0 & 1 \end{pmatrix}, \quad (1.2)$$

and we have used the standard notation $c_{ij} \equiv \cos \theta_{ij}$, $s_{ij} \equiv \sin \theta_{ij}$ and

$$Q = \text{Diag}(1, e^{i\alpha_{21}/2}, e^{i\alpha_{31}/2}). \quad (1.3)$$

Sometimes a different parametrisation of the Majorana phases is being used, namely $Q' = \text{Diag}(e^{-i\beta_1/2}, e^{-i\beta_2/2}, 1)$. Obviously, $Q = e^{i\beta_1/2}Q'$, with $\alpha_{21} = \beta_1 - \beta_2$ and $\alpha_{31} = \beta_1$ ¹.

The neutrino oscillation data, accumulated over many years, allowed to determine the parameters which drive the solar and atmospheric neutrino oscillations, $\Delta m_{\odot}^2 \equiv \Delta m_{21}^2$, θ_{12} and $|\Delta m_A^2| \equiv |\Delta m_{31}^2| \cong |\Delta m_{32}^2|$, θ_{23} , with a rather high precision (see, e.g., [1]). Furthermore, there were spectacular developments in the last year in what concerns the angle θ_{13} . In June of 2011 the T2K collaboration reported [3] evidence at 2.5σ for a non-zero value of θ_{13} . Subsequently the MINOS [4] and Double Chooz [5] collaborations also reported evidence for $\theta_{13} \neq 0$, although with a smaller statistical significance. Global analysis of the neutrino oscillation data, including the data from the T2K and MINOS experiments, performed in [6], showed that actually $\sin \theta_{13} \neq 0$ at $\geq 3\sigma$. In March of 2012 the first data of the Daya Bay reactor antineutrino experiment on θ_{13} were published [7]. The value of $\sin^2 2\theta_{13}$ was measured with a rather high precision and was found to be different from zero at 5.2σ :

$$\sin^2 2\theta_{13} = 0.092 \pm 0.016 \pm 0.005, \quad 0.04 \leq \sin^2 2\theta_{13} \leq 0.14, \quad 3\sigma, \quad (1.4)$$

where we have given also the 3σ interval of allowed values of $\sin^2 2\theta_{13}$. Subsequently, the RENO experiment reported a 4.9σ evidence for a non-zero value of θ_{13} [8], compatible with the Daya Bay result:

$$\sin^2 2\theta_{13} = 0.113 \pm 0.013 \pm 0.019. \quad (1.5)$$

¹For "technical" reasons related to the fitting code we will employ, we will use in what follows quite often the parametrisation given by Q' .

Parameter	best-fit ($\pm 1\sigma$)	3σ
Δm_{\odot}^2 [10^{-5} eV ²]	7.62 ± 0.19	7.12 - 8.20
$ \Delta m_A^2 $ [10^{-3} eV ²]	$2.53^{+0.08}_{-0.10}$	2.26 - 2.77
	$-(2.40^{+0.10}_{-0.07})$	-(2.15-2.68)
$\sin^2 \theta_{12}$	$0.320^{+0.015}_{-0.017}$	0.27 - 0.37
$\sin^2 \theta_{23}$	$0.49^{+0.08}_{-0.02}$	0.39-0.64
	$0.53^{+0.05}_{-0.07}$	
$\sin^2 \theta_{13}$	$0.026^{+0.003}_{-0.004}$	0.015-0.036
	$0.027^{+0.003}_{-0.004}$	0.016-0.037

Table 1: The best-fit values and 3σ allowed ranges of the 3-neutrino oscillation parameters derived from a global fit of the current neutrino oscillation data, including the Daya Bay and RENO results (from [10]). These values are obtained using the “new” [11] reactor $\bar{\nu}_e$ fluxes. If two values are given the first one corresponds to normal hierarchy and the second one to inverted hierarchy.

The results on θ_{13} described above will have far reaching implications for the program of future research in neutrino physics (see, e.g., [9]).

A recent global analysis of the current neutrino oscillation data, in which the Daya Bay and RENO results on θ_{13} are also included, was published [10]. In Table 1 we show the best fit values and the 99.73% CL allowed ranges of Δm_{21}^2 , $\sin^2 \theta_{12}$, $|\Delta m_{31(32)}^2|$, $\sin^2 \theta_{23}$ and $\sin^2 \theta_{13}$, found in [10].

Stimulated by the fact that all three angles in the PMNS matrix are determined with a relatively high precision, we report in the present article an attempt to construct a unified model of flavour, which describes correctly the quark and charged lepton masses, the mixing and CP violation in the quark sector, the mixing in the lepton sector, including the relatively large value of the angle θ_{13} , and provides predictions for the light neutrino masses compatible with the existing relevant data and constraints. The model is supersymmetric and is based on the symmetry group $SU(5) \times T'$. It includes three right-handed (RH) neutrino fields N_{lR} , $l = e, \mu, \tau$, which possess a Majorana mass term. The light neutrino masses are generated by the type I see-saw mechanism [12] and are naturally small. The corresponding Majorana mass term of the left-handed flavour neutrino fields $\nu_{lL}(x)$, $l = e, \mu, \tau$, is diagonalised by a unitary matrix which, up to a diagonal phase matrix, is of the tri-bimaximal form [13]:

$$U_{\text{TBM}} = \begin{pmatrix} \sqrt{2/3} & \sqrt{1/3} & 0 \\ -\sqrt{1/6} & \sqrt{1/3} & -\sqrt{1/2} \\ -\sqrt{1/6} & \sqrt{1/3} & \sqrt{1/2} \end{pmatrix}. \quad (1.6)$$

In order to account for the current data on the neutrino mixing, and more specifically, for the fact that $\theta_{13} \neq 0$, U_{TBM} has to be “corrected”. The requisite correction is provided by the unitary matrix originating from the diagonalisation of the charged lepton mass matrix M_e (for a general discussion of such corrections see, e.g., [14–16]). Since the model is based on the $SU(5)$ GUT symmetry, the charged lepton mass matrix M_e is related to the down-quark mass matrix M_d . As a consequence, in particular, of the connection between M_e and M_d , the smallest angle in the neutrino mixing matrix θ_{13} , is related to the Cabibbo angle θ^c : $\sin^2 \theta_{13} \cong C^2(\sin^2 \theta^c)/2 \cong (\sin^2 \theta^c)/2.5$, where $C \cong 0.9$ is a constant determined from the fit.

The down-quark mass matrix M_d , and the charged lepton mass matrix M_e , by construction are neither diagonal nor CP conserving. The matrix M_e is the only source of CP violation in the lepton sector. Actually, the CP violation predicted by the model in the quark and lepton sectors is entirely geometrical in origin. This aspect of the $SU(5) \times T'$ model we propose is a consequence, in particular, of one of the special properties of the group T' ², namely, that its group theoretical Clebsch-Gordan (CG) coefficients are intrinsically complex [19]. The idea to use the complexity of the Clebsch-Gordan (CG) coefficients of T' to generate the requisite CP violation in the quark sector and a related CP violation in the lepton sector was pioneered in [20]. For the class of models where the CP violation is geometrical in origin, it is essential to provide a solution to the vacuum alignment problem for which all the flavon vevs are real. In this paper we present a solution of this problem for the models based on the $SU(5) \times T'$ symmetry.

Let us note finally that a model of flavour based on the symmetry group $SU(5) \times T'$ was proposed, to our knowledge, first in [21] and its properties were further elaborated in [20] and [22]. Although some generic features, as like the connection between the reactor mixing angle θ_{13} and the Cabibbo angle θ^c , which are based on the underlying $SU(5)$ symmetry, are present both in the model constructed in [20, 21] and in the model presented here, the detailed structure and the quantitative predictions of the two models are very different. The quark, charged lepton, RH neutrino mass matrices and the matrix of the neutrino Yukawa couplings have different forms in the two models. This leads to considerable differences in the predictions for various observables. In the quark sector, for instance, the value of the CKM phase we find is in much better agreement with experimental data. More importantly, in the model proposed in [20, 21], the reactor mixing angle θ_{13} is predicted to have the value $\sin \theta_{13} \cong \sin \theta^c / (3\sqrt{2}) \cong 0.016$, which is ruled out by the current data on θ_{13} . In contrast, due to non-standard $SU(5)$ Clebsch-Gordan relations between the down-type quark and the charged lepton Yukawa couplings [16, 23], we get a realistic value for this angle. Moreover, in the model we propose both neutrino mass spectra with normal and inverted ordering are possible, while the model developed in [20, 21] admits only neutrino mass spectrum with normal ordering [22].

The paper is organized as follows. Section 2 is a brief overview of the considered model. In section 3 we discuss the quark and charged lepton sector including a χ^2 fit to the experimental data. Section 4 is completely devoted to the neutrino sector. There we describe in detail the predictions for the mixing parameters (including CP violating phases), the mass spectra and observables such as the sum of the neutrino masses, the effective Majorana mass for $(\beta\beta)_{0\nu}$ -Decay and the rephasing invariant related to the Dirac phase in the PMNS matrix, J_{CP} . We summarize and conclude in section 5. In the Appendix we discuss the properties of the discrete group T' , the messenger sector which generates the effective operators for the Yukawa couplings, and the superpotential, solving the flavon vacuum alignment problem.

2 Matter, Higgs and Flavon Field Content of the Model

We consider a unified model of flavour with $SU(5)$ as gauge group and T' as discrete family symmetry. A rather large shaping symmetry, $Z_{12} \times Z_8^3 \times Z_6^2 \times Z_4$, is needed to solve the vacuum alignment issue and forbids unwanted terms and couplings in the superpotential (specifically in the renormalisable one as described in Appendix B, as well as in the effective one after integrating out heavy messenger fields). We further impose an additional $U(1)_R$ symmetry, the

²There have been also T' models without a GUT embedding, e.g. [17, 18].

	T_3	T_a	\bar{F}	N	$H_5^{(1)}$	$H_5^{(2)}$	$H_5^{(3)}$	$\bar{H}_5^{(1)}$	$\bar{H}_5^{(2)}$	$\bar{H}_5^{(3)}$	\bar{H}_5''	H_{24}''	\tilde{H}_{24}''
$SU(5)$	10	10	$\bar{5}$	1	5	5	5	$\bar{5}$	$\bar{5}$	$\bar{5}$	$\bar{5}$	24	24
T'	1	2	3	3	1	1	1	1	1	1	1''	1''	1''
$U(1)_R$	1	1	1	1	0	0	0	0	0	0	0	0	0
Z_{12}^u	2	11	1	9	8	8	2	9	3	6	3	0	3
Z_8^d	4	0	2	6	0	4	0	1	4	7	7	4	2
Z_8^ν	7	6	2	0	2	6	4	1	1	5	7	4	0
Z_8	0	5	2	2	0	0	6	0	0	6	6	4	2
Z_6	5	0	1	0	2	5	2	2	0	2	2	0	0
Z_6'	2	3	1	0	2	5	2	5	0	2	2	0	0
Z_4	3	3	0	0	2	0	2	0	1	1	0	0	1

Table 2: Matter and Higgs field content of the model including quantum numbers.

continuous generalisation of the usual R -parity. In this section we describe the matter, the Higgs and the flavon content of the model. The messenger fields and auxiliary flavons used for the flavon superpotential are discussed in the Appendix.

The model includes the three generations of matter fields in the usual $\bar{5}$ and 10 , representations of $SU(5)$, $\bar{F} = (d^c, L)_L$ and $T = (q, u^c, e^c)_L$ and three heavy right-handed Majorana neutrino fields N , singlets under $SU(5)$. The light active neutrino masses are generated through the type I seesaw mechanism [12]. Furthermore we introduce a number of copies of Higgs fields in the 5 and $\bar{5}$ representation of $SU(5)$ which contain as linear combinations the two Higgs doublets of the MSSM. To get realistic mass ratios between down-type quarks and charged leptons [23] and to get a large reactor mixing angle [16] we have introduced Higgs fields in the adjoint representation of $SU(5)$ which are as well responsible for breaking the GUT group.

The matter and Higgs fields including their transformation properties under all imposed symmetries are summarised in Tab. 2. Note that the right-handed neutrinos N and the five-dimensional matter representations are organised in T' triplets, while the ten-plets are organised in a doublet and a singlet. On the one hand this will give us tri-bimaximal mixing (TBM) in the neutrino sector before considering corrections from the charged lepton sector and on the other hand the complex Clebsch–Gordan coefficients for the doublets will give us CP violation in the quark and in the lepton sector finally.

There are 13 flavons, which will give us the desired structure for the Yukawa couplings that will be discussed in the next section. First of all we have three triplets which will develop vevs into two different directions in flavour space,

$$\langle \phi \rangle = \begin{pmatrix} 0 \\ 0 \\ 1 \end{pmatrix} \phi_0, \quad \langle \tilde{\phi} \rangle = \begin{pmatrix} 0 \\ 0 \\ 1 \end{pmatrix} \tilde{\phi}_0, \quad \langle \xi \rangle = \begin{pmatrix} 1 \\ 1 \\ 1 \end{pmatrix} \xi_0. \quad (2.1)$$

The first two flavons will be relevant for the quark and the charged lepton sector and the third one couples only to the neutrino sector.

Then we have introduced four complex T' doublets. Notice that this spinorial representations of the T' group are essential since, having complex Clebsch-Gordan coefficients (see Appendix A), it is responsible of the CP violation in both quark and charged lepton sector. We assume that CP is conserved on the fundamental level (all couplings are real) and all flavon vevs are real.

	$\tilde{\phi}$	$\tilde{\psi}''$	$\tilde{\psi}'$	$\tilde{\zeta}''$	$\tilde{\zeta}'$	ϕ	ψ''	ψ'	ζ''	ζ'	ξ	ρ	$\tilde{\rho}$
$SU(5)$	1	1	1	1	1	1	1	1	1	1	1	1	1
T'	3	2''	2'	1''	1'	3	2''	2'	1''	1'	3	1	1
$U(1)_R$	0	0	0	0	0	0	0	0	0	0	0	0	0
Z_{12}^u	0	3	9	0	0	6	3	9	6	0	6	6	6
Z_8^d	0	0	0	0	0	2	1	7	6	4	4	4	4
Z_8^ν	4	1	7	0	0	2	7	1	6	4	0	0	0
Z_8	4	7	5	4	0	2	5	3	6	4	4	4	4
Z_6	4	4	2	4	2	0	3	3	0	0	0	0	0
Z'_6	4	4	2	4	2	3	0	0	0	0	0	0	0
Z_4	0	2	2	0	0	0	3	1	2	0	0	0	0

Table 3: Flavon fields coupling to the matter sector including their quantum numbers. In fact, ζ' does not couple directly to the matter fields, but it behaves very similar like the other flavons and not like the auxiliary flavons ϵ which will be introduced in Appendix C.

In Appendix C we give a superpotential that has the desired flavon vev directions as a solution and also fixes the phases of the vevs up to a few discrete choices. For the doublets we find the vev alignments

$$\begin{aligned}
\langle \psi' \rangle &= \begin{pmatrix} 1 \\ 0 \end{pmatrix} \psi'_0, & \langle \psi'' \rangle &= \begin{pmatrix} 0 \\ 1 \end{pmatrix} \psi''_0, \\
\langle \tilde{\psi}' \rangle &= \begin{pmatrix} 1 \\ 0 \end{pmatrix} \tilde{\psi}'_0, & \langle \tilde{\psi}'' \rangle &= \begin{pmatrix} 0 \\ 1 \end{pmatrix} \tilde{\psi}''_0
\end{aligned} \tag{2.2}$$

Furthermore we have introduced six flavons in one-dimensional representations of T' which receive all non-vanishing (and real) vevs

$$\langle \zeta' \rangle = \zeta'_0, \quad \langle \zeta'' \rangle = \zeta''_0, \quad \langle \tilde{\zeta}' \rangle = \tilde{\zeta}'_0, \quad \langle \tilde{\zeta}'' \rangle = \tilde{\zeta}''_0, \quad \langle \rho \rangle = \rho_0, \quad \langle \tilde{\rho} \rangle = \tilde{\rho}_0. \tag{2.3}$$

All flavons including their quantum numbers are summarised in Tab. 3. As we will see soon the flavon field ζ' does not directly couple to the matter sector. Nevertheless, we mention it here because it behaves differently than the auxiliary ϵ flavons which we have introduced to get the desired alignment and make all vevs real, see Appendix C.

3 The Quark and Charged Lepton Sector

In this section we describe the superpotential of the quark and charged lepton content of the chiral superfields of the model under study. We will consider the three generations of matter fields in the usual $\bar{\mathbf{5}}$ and $\mathbf{10}$, five and ten- dimensional, representations of $SU(5)$, $\bar{F} = (d^c, L)_L$ and $T = (q, u^c, e^c)_L$. The elements of the Yukawa coupling matrices are generated dynamically through a number of effective operators which structure is tightly related to the matter fields assignment under the T' discrete symmetry. Indeed the Yukawa coupling matrices can be written only after the breaking of the T' discrete symmetry. As will be clear soon, in this description CP violation in the quark and charged lepton sector is entirely due to geometrical origin, specifically from the use of the spinorial representation of the T' group. Finally, in this section we will

present a χ^2 fit analysis that has been performed by us to get the low energy masses and mixing parameters in the quark and charged lepton sector. We show as well that the simple CKM phase sum rule from [24] can be applied here.

3.1 Effective Operators and Yukawa Matrices

Before we come to the effective operators which will give us the Yukawa couplings we first fix the conventions used for the Yukawa matrices. Throughout this paper we will use the RL convention, i.e.,

$$-\mathcal{L} = Y_{ij} \overline{f_R^i} f_L^j H + \text{H.c.} \quad (3.1)$$

or in other words we have to diagonalise the combination $Y^\dagger Y$. Keep also in mind that $\bar{F} = (d^c, L)_L$ and $T = (q, u^c, e^c)_L$.

We restrict ourselves to effective operators up to mass dimension seven. The dimension seven operators have coefficients of the order of 10^{-5} or smaller (see our fit results in Tab. 5). Higher dimensional operators hence can be expected to give only negligible corrections.

After integrating out the heavy messenger fields, see Appendix B, we obtain the effective operators

$$\begin{aligned} \mathcal{W}_{Y_u} = & y_{33} H_5^{(1)} T_3 T_3 + \frac{y_{23}}{\Lambda^2} (T_a \tilde{\phi})_{2'} H_5^{(2)} (T_3 \tilde{\psi}'')_{2''} + \frac{y_{22}}{\Lambda^3} (T_a \tilde{\psi}'')_3 (H_5^{(1)} \tilde{\zeta}')_{1'} (T_a \tilde{\psi}'')_3 \\ & + \frac{y_{21}}{\Lambda^4} (T_a \tilde{\phi})_{2'} (H_5^{(1)} \tilde{\zeta}')_{1'} (\tilde{\psi}' (T_a \tilde{\psi}')_3)_{2'} + \frac{y_{11}}{\Lambda^4} ((T_a \tilde{\phi})_2 \tilde{\zeta}'')_{2''} H_5^{(3)} (\tilde{\zeta}'' (T_a \tilde{\phi})_{2'})_{2'} , \end{aligned} \quad (3.2)$$

which give the up-type quark Yukawa matrices after the flavons developed their vevs. Here Λ stands for the messenger scale suppressing the non-renormalisable operators. We have also given the T' contractions as indices on the round brackets. Note that in general there are many different contractions possible (for T' and to a less degree for $SU(5)$) which give different results. Nevertheless, we have specified in Appendix B the fields mediating the non-renormalisable operators which transform in a specific way under T' such that we pick up only the contractions which we want.

Multiplying the T' and $SU(5)$ indices out we obtain for the up-type quark Yukawa matrix at the GUT scale (which is roughly equal to the scale of T' breaking)

$$Y_u = \begin{pmatrix} \bar{\omega} a_u & i b_u & 0 \\ i b_u & c_u & \omega d_u \\ 0 & \omega d_u & e_u \end{pmatrix} , \quad (3.3)$$

where $\omega = (1 + i)/\sqrt{2}$ and $\bar{\omega} = (1 - i)/\sqrt{2}$. The parameters a_u, b_u, c_u, d_u and e_u are (real) functions of the underlying parameters. Note at this point, that the phases of the flavon vevs have to be fixed. Otherwise the coefficients in the Yukawa matrix are complex parameters and we would not be able to make definite predictions anymore.

For the down-type quarks and charged leptons (remember that those two sectors are closely related in $SU(5)$) we find for the superpotential

$$\begin{aligned} \mathcal{W}_{Y_{d,e}} = & \frac{y_{33}}{\Lambda^2} ((\bar{H}_5^{(2)} \bar{F})_3 \phi)_{1'} (H_{24}'' T_3)_{1''} + \frac{y_{22}}{\Lambda^3} ((\phi T_a)_{2'} H_{24}'')_2 (\psi' (\bar{H}_5^{(1)} \bar{F})_3)_2 \\ & + \frac{y_{12}}{\Lambda^4} (((T_a \tilde{H}_{24}'')_{2''} (\bar{F} \psi')_{2''})_3 \psi')_{2''} (\bar{H}_5^{(3)} \psi')_{2'} + \frac{y_{21}}{\Lambda^4} ((\bar{F} \psi')_{2''} (\zeta'' \bar{H}_5^{(1)})_{1''} \zeta'')_2 (T_a \phi)_2 \\ & + \frac{y_{11}}{\Lambda^4} ((\bar{F} \psi'')_{2'} (H_{24}'' \psi'')_{2'} \bar{H}_5^{(1)})_{1'} (T_a \psi'')_{1''} , \end{aligned} \quad (3.4)$$

where we have again specified the T' contractions. From this superpotential and considering the correct $SU(5)$ contractions, which we could not display here for the sake of readability, we get the down-type quark and charged lepton Yukawa matrices

$$Y_d = \begin{pmatrix} \omega a_d & i b'_d & 0 \\ \bar{\omega} b_d & c_d & 0 \\ 0 & 0 & d_d \end{pmatrix} \quad \text{and} \quad Y_e = \begin{pmatrix} -\frac{3}{2} \omega a_d & \bar{\omega} b_d & 0 \\ 6 i b'_d & 6 c_d & 0 \\ 0 & 0 & -\frac{3}{2} d_d \end{pmatrix}, \quad (3.5)$$

where a_d, b_d, b'_d, c_d and d_d are (real) functions of the underlying parameters.

Note that the prediction from the minimal $SU(5)$ model $Y_d = Y_e^T$ is broken. Indeed it has to be broken to get realistic fermion masses. For the second generation this is known for a long time [25]. In some recent work [23] some new relations to fix this issue were proposed. From those we will use here $y_\tau/y_b = -3/2$ and $y_\mu/y_s \approx 6$. Furthermore it was shown in [16] (see also [26]) that those new $SU(5)$ Clebsch–Gordan coefficients might also give a large reactor neutrino mixing angle θ_{13} . For the current paper we have chosen one of the possible combinations given in [16] but we remark that in principle also other combinations are still possible which might be realised in another unified flavour model with a similar good fit to the fermion masses and mixing angles.

3.2 Fit Results and the CKM Phase Sum Rule

In the last section we have discussed the structure of the Yukawa matrices in the quark and the charged lepton sector. These matrices have five free parameters, which in principle can be fitted to the low-energy mass and mixing parameters using the renormalisation group. But doing so one has to take into account SUSY threshold corrections [27] which modify the masses and mixing angles significantly. For example without including them the GUT scale Yukawa coupling ratio y_τ/y_b would be roughly 1.3 which is not close to the usual GUT prediction of 1, see, for example, [23, 28].

Hence, neglecting the SUSY threshold corrections a fit to the low-energy parameters is usually bad. In [29] the approximate matching conditions at the SUSY scale, M_{SUSY} ,

$$y_{e,\mu,\tau}^{\text{SM}} = (1 + \epsilon_l \tan \beta) y_{e,\mu,\tau}^{\text{MSSM}} \cos \beta, \quad (3.6)$$

$$y_{d,s}^{\text{SM}} = (1 + \epsilon_q \tan \beta) y_{d,s}^{\text{MSSM}} \cos \beta, \quad (3.7)$$

$$y_b^{\text{SM}} = (1 + (\epsilon_q + \epsilon_A) \tan \beta) y_b^{\text{MSSM}} \cos \beta, \quad (3.8)$$

for the Yukawa couplings and

$$\theta_{i3}^{\text{SM}} = \frac{1 + \epsilon_q \tan \beta}{1 + (\epsilon_q + \epsilon_A) \tan \beta} \theta_{i3}^{\text{MSSM}}, \quad (3.9)$$

$$\theta_{12}^{\text{SM}} = \theta_{12}^{\text{MSSM}}, \quad (3.10)$$

$$\delta_{\text{CKM}}^{\text{SM}} = \delta_{\text{CKM}}^{\text{MSSM}}, \quad (3.11)$$

for the quark mixing parameters were given, where the SUSY threshold corrections are parameterised in terms of the three parameters ϵ_l, ϵ_q and ϵ_A . We will adopt this parameterisation neglecting ϵ_l , which is usually one order smaller than ϵ_q [28]. Furthermore we want to assume, that SUSY is broken similar to the constrained MSSM scenario with a positive μ parameter and hence the recently proposed GUT scale Yukawa coupling ratios $y_\tau/y_b = 3/2$ and $y_\mu/y_s \approx 6$ are preferred [23].

Parameter	Value
a_u	$5.81 \cdot 10^{-6}$
b_u	$-9.96 \cdot 10^{-5}$
c_u	$-8.55 \cdot 10^{-4}$
d_u	$1.99 \cdot 10^{-2}$
e_u	0.525
a_d	$-2.82 \cdot 10^{-5}$
b_d	$-5.73 \cdot 10^{-4}$
b'_d	$-5.09 \cdot 10^{-4}$
c_d	$2.50 \cdot 10^{-3}$
d_d	$1.82 \cdot 10^{-1}$
$\epsilon_q \tan \beta$	0.1788
$\epsilon_A \tan \beta$	-0.0001

Table 4: Values of the effective parameters of the quark and charged lepton Yukawa matrices for $\tan \beta = 35$ and $M_{\text{SUSY}} = 750$ GeV. The two parameters ϵ_q and ϵ_A parameterise the SUSY threshold corrections. The numerical values are determined from a χ^2 -fit to experimental data with a lowest χ^2 per degree of freedom of 2.76.

We have fixed the SUSY scale to 750 GeV, the GUT scale to 2×10^{16} GeV and $\tan \beta$ to 35. Therefore we have to fit the ten parameters in the Yukawa matrices and the two parameters from the SUSY threshold corrections to the thirteen low energy observables in the quark and the charged lepton sector (nine masses, three mixing angles and one phase), so that we have one prediction (degree of freedom).

The RGE running and diagonalisation of the matrices was done using the REAP package [30]. Performing a χ^2 fit we have found as minimum the results listed in Tab. 4 for the parameters and in Tab. 5 and in Fig. 1 we have presented the predictions for the low energy observables compared to the experimental results. Note that we have assumed an uncertainty of 3% on the Yukawa couplings for the charged leptons. Their experimental uncertainty is much smaller, so that their theoretical uncertainty (Accuracy of RGEs, neglecting SUSY threshold corrections for the leptons, NLO effects, ...) is much bigger, which we estimate to be 3%.

We find very good agreement between our model and experimental data with a minimal χ^2 per degree of freedom of 2.76. In fact this agreement is not accidental. We have chosen the $SU(5)$ coefficients such that, we expect good agreement and we have also enough free parameters to fix the mixing angles. In other words one could determine the eigenvalues and mixing angles from the data and then the CKM phase would be a prediction. But as we will demonstrate now, the choice for our phases in the Yukawa matrices was done in such a way, that we can expect a good prediction for the CKM phase as well.

We will show in the following that the sum rule given in [24] can be used here. To apply the sum rule we have to find approximate expressions for the complex mixing angles (see [24] for the notation used in the rest of this subsection). We find at leading order for the mixing angles and phases

$$\theta_{12}^d e^{-i\delta_{12}^d} = \left| \frac{b_d}{c_d} \right| e^{-i\frac{7\pi}{4}}, \quad \theta_{13}^d = \theta_{23}^d = 0, \quad (3.12)$$

Quantity (at $m_t(m_t)$)	Experiment	Model	Deviation
y_τ in 10^{-2}	1.00	0.99	-0.388
y_μ in 10^{-4}	5.89	5.90	0.044
y_e in 10^{-6}	2.79	2.79	-0.003
y_b in 10^{-2}	1.58 ± 0.05	1.57	-0.157
y_s in 10^{-4}	2.99 ± 0.86	2.57	-0.484
y_s/y_d	18.9 ± 0.8	18.9	-0.012
y_t	0.936 ± 0.016	0.936	0.0001
y_c in 10^{-3}	3.39 ± 0.46	2.79	-1.317
y_u in 10^{-6}	$7.01^{+2.76}_{-2.30}$	7.01	-0.0003,
θ_{12}^{CKM}	$0.2257^{+0.0009}_{-0.0010}$	0.2257	-0.0107
θ_{23}^{CKM}	$0.0415^{+0.0011}_{-0.0012}$	0.0416	0.1268
θ_{13}^{CKM}	0.0036 ± 0.0002	0.0036	0.2043
δ_{CKM}	$1.2023^{+0.0786}_{-0.0431}$	1.2610	0.7465

Table 5: Fit results for the quark Yukawa couplings and mixing and the charged lepton Yukawa couplings at low energy compared to experimental data. The values for the Yukawa couplings are extracted from [31], the ratio y_s/y_d is taken from [32] and the CKM parameters from [1]. Note that the experimental uncertainty on the charged lepton Yukawa couplings are negligible small and we have assumed a relative uncertainty of 3 % for them. The χ^2 per degree of freedom is 2.76. A pictorial representation of the agreement between our predictions and experiment can be found as well in Fig. 1.

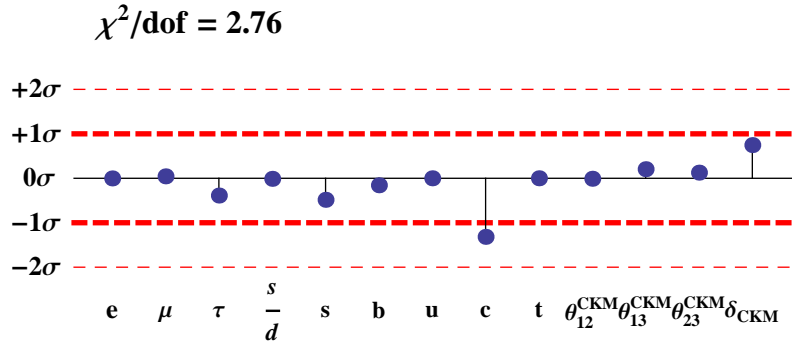


Figure 1: Pictorial representation of the deviation of our predictions from low energy experimental data for the charged lepton Yukawa couplings and quark Yukawa couplings and mixing parameters. The deviations of the charged lepton masses are given in 3% while all other deviations are given in units of standard deviations σ .

$$\theta_{12}^u e^{-i\delta_{12}^u} \approx \left| \frac{b_u}{\sqrt{2}c_u} \right| e^{-i\frac{5\pi}{4}}, \quad \theta_{23}^u e^{-i\delta_{23}^u} = \left| \frac{d_u}{e_u} \right| e^{-i\frac{5\pi}{4}}, \quad \theta_{13}^u e^{-i\delta_{13}^u} = \left| \frac{b_u d_u}{e_u^2} \right| e^{-i\frac{\pi}{4}}, \quad (3.13)$$

where we have used for θ_{12}^u that $d_u^2 \approx -1/2c_u$ and $e_u \approx 0.5$ from our fit. So we see that δ_{12}^u is not simply $\pi/2$ as one would expect from a quick first inspection. Note also that the phase sum rule was derived for $\theta_{13}^u = \theta_{13}^d = 0$, which is not exactly true in our case for θ_{13}^u . But in fact it is sufficient, that $\theta_{13}^u \ll \theta_{12}^u \theta_{23}^u$ which is fulfilled here.

The angle α in the CKM unitarity triangle is experimentally measured to be $\alpha = (90.7_{-2.9}^{+4.5})^\circ$ [33] for which the sum rule

$$\alpha \approx \delta_{12}^d - \delta_{12}^u, \quad (3.14)$$

was given in [24]. Plugging in our approximate analytical expressions for $\delta_{12}^{d/u}$, eqs. (3.12) and (3.13), we find that $\alpha \approx \pi/2$ and our model is in good agreement with experimental data as we have also seen it before from our numerical fit.

4 Neutrino Sector

The model includes three heavy right-handed Majorana neutrino fields N which are singlets under $SU(5)$ and a triplet under T' . Through the type I seesaw mechanism [12] we generate light neutrino masses. The neutrino sector is described by the following terms in the superpotential

$$\mathcal{W}_\nu = \lambda_1 N N \xi + N N (\lambda_2 \rho + \lambda_3 \tilde{\rho}) + \frac{y_\nu}{\Lambda} (N \bar{F})_1 (H_5^{(2)} \rho)_1 + \frac{\tilde{y}_\nu}{\Lambda} (N \bar{F})_1 (H_5^{(2)} \tilde{\rho})_1, \quad (4.1)$$

where we have given the T' contractions as indices at the brackets for non-renormalisable terms. Note that the contraction of three triplets in general is not unique, see also Tab. 7, because the product of two triplets contains a symmetric and an antisymmetric triplet. But since we multiply here two N with each other only the symmetric combination gives a non-vanishing contribution. In the following we will discuss the phenomenological implications of this superpotential (including corrections from the charged lepton sector).

4.1 The Neutrino Mass Spectrum

From eq. (4.1) we obtain for the mass matrix for the right-handed neutrinos and the Dirac neutrino mass matrix

$$M_R = \begin{pmatrix} 2Z + X & -Z & -Z \\ -Z & 2Z & -Z + X \\ -Z & -Z + X & 2Z \end{pmatrix}, \quad M_D = \begin{pmatrix} 1 & 0 & 0 \\ 0 & 0 & 1 \\ 0 & 1 & 0 \end{pmatrix} \frac{\rho'}{\Lambda}, \quad (4.2)$$

where X , Z and ρ' are real parameters depending on the couplings and the vevs in eq. (4.1). The right-handed neutrino mass matrix M_R is diagonalised by the tri-bimaximal mixing (TBM) matrix [13]

$$U_{\text{TBM}} = \begin{pmatrix} \sqrt{2/3} & \sqrt{1/3} & 0 \\ -\sqrt{1/6} & \sqrt{1/3} & -\sqrt{1/2} \\ -\sqrt{1/6} & \sqrt{1/3} & \sqrt{1/2} \end{pmatrix}, \quad (4.3)$$

such that the heavy RH neutrino masses read:

$$U_{\text{TBM}}^T M_R U_{\text{TBM}} = D_N = \text{Diag}(3Z + X, X, 3Z - X) = \text{Diag}(M_1 e^{i\phi_1}, M_2 e^{i\phi_2}, M_3 e^{i\phi_3}), \quad M_{1,2,3} > 0, \quad (4.4)$$

where

$$M_1 = |X + 3Z| \equiv |X| |1 + \alpha e^{i\phi}|, \quad \phi_1 = \arg(X + 3Z) \quad (4.5)$$

$$M_2 = |X|, \quad \phi_2 = \arg(X) \quad (4.6)$$

$$M_3 = |X - 3Z| \equiv |X| |1 - \alpha e^{i\phi}|, \quad \phi_3 = \arg(3Z - X). \quad (4.7)$$

Here $\alpha \equiv |3Z/X| > 0$ and $\phi \equiv \arg(Z) - \arg(X)$. Since X and Z are real parameters, the phases ϕ_1, ϕ_2, ϕ_3 and ϕ take values 0 or π . A light neutrino Majorana mass term is generated after electroweak symmetry breaking via the type I see-saw mechanism:

$$M_\nu = -M_D^T M_R^{-1} M_D = U_\nu^* \text{Diag}(m_1, m_2, m_3) U_\nu^\dagger, \quad (4.8)$$

where

$$U_\nu = i U_{\text{TBM}} \text{Diag}(e^{i\phi_1/2}, e^{i\phi_2/2}, e^{i\phi_3/2}) \equiv i U_{\text{TBM}} \tilde{Q}, \quad \tilde{Q} \equiv \text{Diag}(e^{i\phi_1/2}, e^{i\phi_2/2}, e^{i\phi_3/2}), \quad (4.9)$$

and $m_{1,2,3} > 0$ are the light neutrino masses,

$$m_i = \left(\frac{\rho'}{\Lambda}\right)^2 \frac{1}{M_i}, \quad i = 1, 2, 3. \quad (4.10)$$

The phase factor i in eq. (4.9) corresponds to an unphysical phase and we will drop it in what follows. Note also that one of the phases ϕ_k , say ϕ_1 , is physically irrelevant since it can be considered as a common phase of the neutrino mixing matrix. In the following we always set $\phi_1 = 0$. This corresponds to the choice $(X + 3Z) > 0$.

The type of the neutrino mass spectrum in the model is determined³ by the value of the phase ϕ . Indeed, as it is not difficult to show, we have:

$$\Delta m_{31}^2 \equiv \Delta m_A^2 = \frac{1}{|X|^2} \left(\frac{\rho'}{\Lambda}\right)^4 \frac{4\alpha \cos \phi}{|1 + \alpha e^{i\phi}|^2 |1 - \alpha e^{i\phi}|^2}. \quad (4.11)$$

Thus, for $\cos \phi = +1$, we get $\Delta m_{31}^2 > 0$, i.e., a neutrino mass spectrum with normal ordering (NO), while for $\cos \phi = -1$ one has $\Delta m_{31}^2 < 0$, i.e., neutrino mass spectrum with inverted ordering (IO). We have also:

$$\Delta m_{21}^2 \equiv \Delta m_\odot^2 = \frac{1}{|X|^2} \left(\frac{\rho'}{\Lambda}\right)^4 \frac{\alpha(\alpha + 2 \cos \phi)}{|1 + \alpha e^{i\phi}|^2}. \quad (4.12)$$

For a given type of neutrino mass spectrum, i.e., for a fixed $\phi = 0$ or π , a constraint on the parameter α can be obtained from the requirement that $\Delta m_{21}^2 > 0$ and from the data on the ratio:

$$r = \frac{\Delta m_\odot^2}{|\Delta m_A^2|} = \frac{1}{4} (\alpha + 2 \cos \phi) (1 - 2\alpha \cos \phi + \alpha^2) = 0.032 \pm 0.006. \quad (4.13)$$

Using the values of α thus found and the value of, e.g., Δm_{21}^2 , one can get (for a given type of the spectrum) the value of the factor in eq. (4.12), $|X|^{-2}(\rho'/\Lambda)^4$. Knowing this factor and α , one can obtain the value of the lightest neutrino mass, which together with the data on Δm_{21}^2

³We are following in this part the similar analysis performed in [34].

and $\Delta m_{31(32)}^2$ allows to obtain the values of the other two light neutrino masses. Knowing the latter one can find also the two ratios of the heavy Majorana neutrino masses.

In the case of NO neutrino mass spectrum ($\phi = 0$), there are two values of α which satisfy equation (4.13) for $r = 0.032$: $\alpha \cong 1.20$ (solution A), and $\alpha \cong 0.79$ (solution B). In the case of solution A, as it is not difficult to show, the phases

$$\phi_2 = 0, \quad \phi_3 = 0, \quad \text{solution A (NO)}, \quad (4.14)$$

and the three neutrino masses have the values:

$$m_1 \cong 4.44 \times 10^{-3} \text{ eV}, m_2 \cong 9.77 \times 10^{-3} \text{ eV}, m_3 \cong 4.89 \times 10^{-2} \text{ eV}, \quad \text{solution A (NO)}. \quad (4.15)$$

Evidently, the spectrum is mildly hierarchical. The ratios of the heavy Majorana neutrino masses read: $M_1/M_3 \cong 11.0$ and $M_2/M_3 \cong 5.0$. Thus, we have $M_3 < M_2 < M_1$.

For solution B we find

$$\phi_2 = 0, \quad \phi_3 = \pi, \quad \text{solution B (NO)}, \quad (4.16)$$

while for the values of the three neutrino masses we get:

$$m_1 \cong 5.89 \times 10^{-3} \text{ eV}, m_2 \cong 1.05 \times 10^{-2} \text{ eV}, m_3 \cong 4.90 \times 10^{-2} \text{ eV}, \quad \text{solution B (NO)}. \quad (4.17)$$

The heavy Majorana neutrino mass ratios are given by: $M_1/M_3 \cong 8.33$ and $M_2/M_3 \cong 4.67$. Therefore also in this case we have $M_3 < M_2 < M_1$.

For the IO spectrum ($\phi = \pi$), we find only one value of α which satisfies eq. (4.13) with $r = 0.032$: $\alpha \cong 2.014$. The phases ϕ_2 and ϕ_3 take the values: $\phi_2 = \pi$, $\phi_3 = 0$. The light neutrino masses read:

$$m_1 \cong 5.17 \times 10^{-2} \text{ eV}, m_2 \cong 5.24 \times 10^{-2} \text{ eV}, m_3 \cong 1.74 \times 10^{-2} \text{ eV}, \quad (\text{IO}), \quad (4.18)$$

i.e., the light neutrino mass spectrum is not hierarchical exhibiting only partial hierarchy. For the heavy Majorana neutrino mass ratios we obtain: $M_1/M_2 \cong 1.014$ and $M_3/M_2 \cong 3.01$. Thus, in this case N_1 and N_2 are quasi-degenerate in mass: $M_1 \cong M_2 < M_3$.

In the Figs. 2 and 3 we present the dependence of the neutrino masses with respect to r for normal and inverted ordering respectively.

4.2 The Mixing Angles and the Dirac and Majorana CP Violation Phase

The PMNS neutrino mixing matrix received contributions from the diagonalisation of the neutrino Majorana mass matrix M_ν and of the charged lepton mass matrix $M_e = v_d Y_e$: $U_{\text{PMNS}} = U_{eL}^\dagger U_\nu$, where U_ν is given in eq. (4.9) with $\tilde{Q} = \text{Diag}(1, e^{i\phi_2/2}, e^{i\phi_3/2})$ and the values of the phases ϕ_2 and ϕ_3 in the cases of NO and IO spectra were specified in the preceding subsection. The matrix of charged lepton Yukawa couplings Y_e , eq. (3.5), and thus M_e , has a block-diagonal form. The unitary matrix U_{eL} diagonalises the Hermitian matrix $M_e^\dagger M_e$: $M_e^\dagger M_e = U_{eL} (M_e^d)^2 U_{eL}^\dagger$, where $M_e^d = \text{diag}(m_e, m_\mu, m_\tau)$, m_l being the mass of the charged lepton l . As a consequence of the block-diagonal form of M_e , the matrix U_{eL} can be parametrised in terms of one mixing angle (θ_{12}^e) and one phase (φ): $U_{eL} = \Phi R_{12}(\theta_{12}^e)$, where $\Phi = \text{diag}(1, e^{i\varphi}, 1)$ and

$$R_{12}(\theta_{12}^e) = \begin{pmatrix} \cos \theta_{12}^e & \sin \theta_{12}^e & 0 \\ -\sin \theta_{12}^e & \cos \theta_{12}^e & 0 \\ 0 & 0 & 1 \end{pmatrix}. \quad (4.19)$$

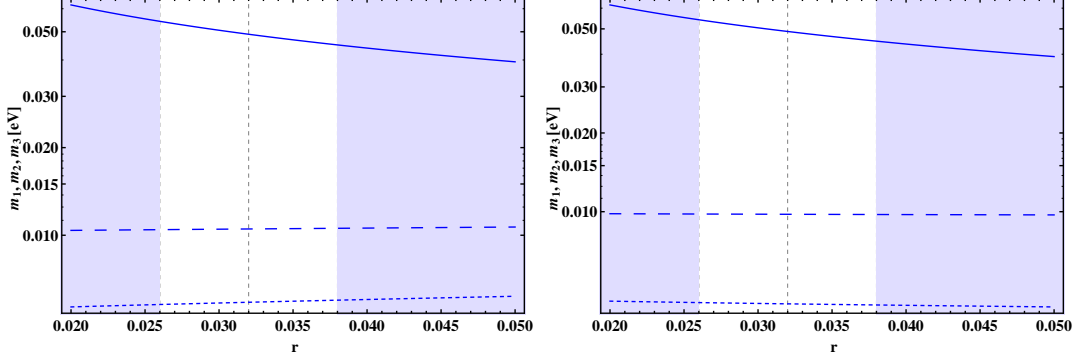


Figure 2: The values of the three light neutrino masses corresponding to the solutions A (left panel) and B (right panel) in the case of NO spectrum, versus r . The gray region is excluded by present oscillation data. The vertical dashed line corresponds to the best fit value for $r = 0.032$. See text for further details.

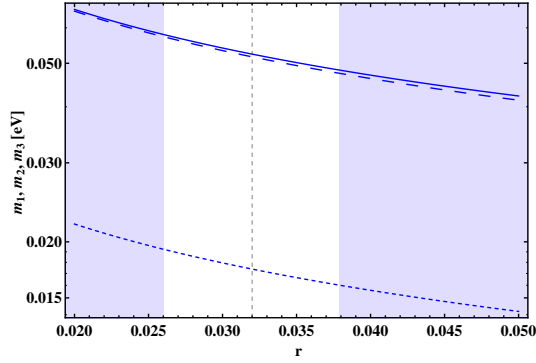


Figure 3: The values of the three light neutrino masses in the case of the solution corresponding to IO spectrum, versus r . The gray region is excluded by present oscillation data. The vertical dashed line corresponds to the best fit value for $r = 0.032$.

Due to the $SU(5)$ symmetry of the model, Y_d and Y_e (and therefore the corresponding down quark and charged lepton mass matrices) are expressed in terms of the same parameters. As a consequence, the angle θ_{12}^e in the model considered is related to the Cabibbo angle $\theta^c \cong 0.226$. Using, for example, the approximate formulas from [16], we find that

$$\theta_{12}^e \cong \left| \frac{b'_d}{b_d} \right| \theta^c \cong 0.9 \theta^c, \quad (4.20)$$

where we have used the values of b'_d and b_d from Table 4.

Comparing next the expressions on the two sides of the equation $M_e^\dagger M_e = U_{eL} (M_e^d)^2 U_{eL}^\dagger$ we get, in particular:

$$e^{-i(\varphi + \frac{\pi}{2})} (m_\mu^2 - m_e^2) \cos \theta_{12}^e \sin \theta_{12}^e = v_d^2 \left(\frac{3}{2} b_d a_d - 36 c_d b'_d \right). \quad (4.21)$$

Using the fit results in Table 4 one can check that the right hand side of the last equation is real and positive. Comparing the phases of the two expressions one concludes that

$$\varphi = \frac{3}{2} \pi. \quad (4.22)$$

In the approximation we are using the PMNS matrix is given by:

$$\tilde{U}_{\text{PMNS}} = \begin{pmatrix} \sqrt{2/3} c_{12}^e + \sqrt{1/6} s_{12}^e e^{-i\varphi} & \sqrt{1/3} c_{12}^e - \sqrt{1/3} s_{12}^e e^{-i\varphi} & \sqrt{1/2} s_{12}^e e^{-i\varphi} \\ \sqrt{2/3} s_{12}^e - \sqrt{1/6} c_{12}^e e^{-i\varphi} & \sqrt{1/3} s_{12}^e + \sqrt{1/3} c_{12}^e e^{-i\varphi} & -\sqrt{1/2} c_{12}^e e^{-i\varphi} \\ -\sqrt{1/6} & \sqrt{1/3} & \sqrt{1/2} \end{pmatrix} \tilde{Q}, \quad (4.23)$$

where $c_{12}^e = \cos \theta_{12}^e$, $s_{12}^e = \sin \theta_{12}^e$ and \tilde{Q} is the diagonal phase matrix defined in eq. (4.9). It follows from the above expression for the PMNS matrix that the angle θ_{13} is given approximately by

$$\sin^2 \theta_{13} \cong \frac{1}{2} C^2 \sin^2 \theta^c \cong \frac{\sin^2 \theta^c}{2.5} \cong 0.02, \quad C \cong 0.9 \quad (4.24)$$

where we took into account the relation in eq. (4.20) and the value of $C \equiv |b'_d/b_d|$.

As was shown in, e.g., [16], the phase φ and the Dirac phase δ in eqs. (1.1) - (1.2) are related (at leading order) as follows:

$$\delta = \varphi + \pi. \quad (4.25)$$

Thus, for the Dirac phase we get from (4.22):

$$\delta = \frac{\pi}{2}. \quad (4.26)$$

Numerically, for $\varphi = 3\pi/2$ and $s_{12}^e = 0.203$ (see eq. (4.20)), the PMNS matrix, eq. (4.23), reads:

$$U_{\text{PMNS}} \cong \begin{pmatrix} 0.804e^{i5.81^\circ} & 0.577e^{-i11.50^\circ} & 0.144e^{-i270.000^\circ} \\ 0.433e^{-i67.85^\circ} & 0.577e^{i78.50^\circ} & -0.692e^{-i270.000^\circ} \\ -0.408 & 0.577 & 0.707 \end{pmatrix} \tilde{Q}. \quad (4.27)$$

Thus, comparing the absolute values of the elements U_{e1} , U_{e2} , $U_{\mu 3}$ and $U_{\tau 3}$ of the PMNS matrix in the standard parametrisation, eq. (1.1), and in eq. (4.27), we have: $c_{12}c_{13} = 0.804$, $s_{12}c_{13} = 0.577$, $s_{23}c_{13} = 0.692$ and $c_{23}c_{13} = 0.707$. Using the predicted value of θ_{13} , eq. (4.24),

these relations allow us to obtain the values of θ_{12} and θ_{23} . We note that the tri-bimaximal mixing value of the solar neutrino mixing angle θ_{12} , which corresponds to $\sin^2 \theta_{12} = 1/3$, is corrected by a quantity which, as it follows from the general form of such corrections [14–16], is determined by the angle θ_{13} and the Dirac phase δ :

$$\sin^2 \theta_{12} \cong \frac{1}{3} + \frac{2\sqrt{2}}{3} \sin \theta_{13} \cos \delta \quad (4.28)$$

where δ is the Dirac phase in the standard parametrisation of the PMNS matrix. As we have seen, to leading order $\delta = \pi/2$. The Majorana phases β_1, β_2 (or α_{21} and α_{31}) are determined, as it follows from eqs. (1.1) and (4.23) (or (4.27)), by the diagonal matrix \tilde{Q} and take CP conserving values. Note, however, that the parametrisation of the PMNS matrix in eq. (4.27) differs from the standard one: it corresponds to one of the several possible parametrisations of the PMNS matrix [15]. Thus, in order to get the values of the Dirac and Majorana phases δ and β_1, β_2 (or α_{21}, α_{31}), of the standard parametrisation of the PMNS matrix, one has to bring the expressions (4.27) in a form which corresponds to the “standard” one in eq. (1.1). This can be done by using the freedom of multiplying the rows of the PMNS matrix with arbitrary phases and by shifting some of the common phases of the columns to a diagonal phase matrix P . The results for the numerical matrix in eq. (4.27) is:

$$U_{\text{PMNS}} \cong \begin{pmatrix} 0.804 & 0.577 & 0.144e^{-i84.25^\circ} \\ -0.433e^{i10.59^\circ} & 0.577e^{-i5.75^\circ} & 0.692 \\ 0.408e^{-i11.56^\circ} & -0.577e^{i5.75^\circ} & 0.707 \end{pmatrix} P \tilde{Q}, \quad (4.29)$$

where $\tilde{Q} = \text{Diag}(1, e^{i\phi_2/2}, e^{i\phi_3/2}) = e^{i\phi_3/2} \text{Diag}(e^{-i\phi_3/2}, e^{-i(\phi_3-\phi_2)/2}, 1)$ and the new phase matrix $P = \text{Diag}(e^{i11.50^\circ}, e^{-i5.81^\circ}, -1)$. Now comparing eq. (4.29) with eq. (1.1) we can obtain the values of the Dirac and the two Majorana phases of the standard parametrisation of the PMNS matrix, predicted by the model. For the Dirac phase we find $\delta \cong 84.3^\circ$. Note that the Majorana phases $\beta_1/2$ and $\beta_2/2$ (or $\alpha_{21}/2$ and $\alpha_{31}/2$) in the standard parametrisation are not CP conserving [22]: due to the matrix P they get CP violating corrections to the CP conserving values 0 and $\pi/2$ or $3\pi/2$.

As we have seen, the value of the Dirac phase δ predicted by the model is close to $\pi/2$. This implies that the magnitude of the CP violation effects in neutrino oscillations, is also predicted to be relatively large. Indeed, the rephasing invariant associated with the Dirac phase [35], $J_{\text{CP}} = \text{Im}(U_{e1}^* U_{\mu 1} U_{e3} U_{\mu 3}^*)$, which determines the magnitude of CP violation effects in neutrino oscillations [36], has the following value:

$$J_{\text{CP}} = 0.0324. \quad (4.30)$$

The values we have obtained for both $\sin \theta_{13}$ and δ are in very good agreement with the numerical results in Table 6 derived using the REAP package [30].

It is possible to derive simple analytic expressions which explain the numerical results ob-

Quantity	Experiment (2σ ranges)	Model
$\sin^2 \theta_{12}$	$0.275 - 0.342$	0.340
$\sin^2 \theta_{23}$	$0.36 - 0.60$	0.490
$\sin^2 \theta_{13}$	$0.015 - 0.032$	0.020
δ	-	84.3°

Table 6: Numerical results for the neutrino sector. The experimental results are taken from [6] apart from the value for θ_{13} which is the DayaBay result [7].

tained above and quoted in Table 6. Indeed, up to corrections of order $(\theta_{12}^e)^2$ we have:

$$\theta_{12} = \arcsin \frac{1}{\sqrt{3}} + \frac{\sqrt{2}}{8}(\theta_{12}^e)^2, \quad (4.31)$$

$$\theta_{13} = \frac{1}{\sqrt{2}}\theta_{12}^e, \quad (4.32)$$

$$\theta_{23} = \frac{\pi}{4} - \frac{1}{4}(\theta_{12}^e)^2, \quad (4.33)$$

$$\delta = \frac{\pi}{2} - \frac{1}{2}\theta_{12}^e, \quad (4.34)$$

$$\beta_1 = 2\pi - 2\theta_{12}^e + \phi_3, \quad (4.35)$$

$$\beta_2 = 2\pi + \theta_{12}^e + \phi_3 - \phi_2, \quad (4.36)$$

where $\theta_{12}^e \cong 0.888\theta^c$. Note that the expression for δ is correct up to $\mathcal{O}(\theta_{12}^e)$ only because it appears always with θ_{13} which is of order θ_{12}^e itself. Numerically, these approximations give for $\theta_{12}^e = 0.2$:

$$\sin^2 \theta_{12} = 0.340, \quad (4.37)$$

$$\sin^2 \theta_{13} = 0.020, \quad (4.38)$$

$$\sin^2 \theta_{23} = 0.490, \quad (4.39)$$

$$\delta = 84.3^\circ, \quad (4.40)$$

$$\beta_1 = 337.1^\circ + \phi_3, \quad (4.41)$$

$$\beta_2 = 11.5^\circ + \phi_3 - \phi_2. \quad (4.42)$$

As we see, the results obtained using the approximate analytic expressions are in very good agreement with those derived in the numerical analysis.

4.3 Predictions for Other Observables in the Neutrino Sector

We derive in this section the predictions for the sum of the neutrino masses and the effective Majorana mass $|\langle m \rangle|$ in neutrinoless double beta decay (see, e.g., [37]) using the standard parameterisation of the PMNS mixing matrix as in (1.2) and the results on the neutrino masses, mixing angles and CPV phases obtained in preceding subsections of this Section.

In the case of solution A for the NO neutrino mass spectrum we get for the sum of the neutrino masses:

$$\sum_{k=1}^3 m_k = 6.31 \times 10^{-2} \text{ eV}, \quad \text{solution A (NO)}. \quad (4.43)$$

In this case we have $\phi_2 = \phi_3 = 0$ (see subsection 4.1) and for the effective Majorana mass we obtain using eqs. (4.15) and (4.29):

$$|\langle m \rangle| = \left| \sum_{k=1}^3 (U_{\text{PMNS}})_{ek}^2 m_k \right| = 4.90 \times 10^{-3} \text{ eV}, \quad \text{solution A (NO)}. \quad (4.44)$$

The same quantities for solution B of the NO spectrum have the values:

$$\sum_{k=1}^3 m_k = 6.54 \times 10^{-2} \text{ eV}, \quad \text{solution B (NO)}, \quad (4.45)$$

and

$$|\langle m \rangle| = 7.95 \times 10^{-3} \text{ eV}, \quad \text{solution B (NO)}, \quad (4.46)$$

where we have used the fact that for solution B we have $\phi_2 = 0$ and $\phi_3 = \pi$. As a consequence, in particular, of the values of $\phi_{2,3}$, the three terms in the expression for $|\langle m \rangle|$ essentially add.

Finally, in the case of IO spectrum we obtain:

$$\sum_{k=1}^3 m_k = 12.1 \times 10^{-2} \text{ eV}, \quad (\text{IO}), \quad (4.47)$$

and

$$|\langle m \rangle| = 2.17 \times 10^{-2} \text{ eV}, \quad (\text{IO}), \quad (4.48)$$

We recall that for the IO spectrum we have $\phi_2 = \pi$ and $\phi_3 = 0$ and there is a partial compensation in $|\langle m \rangle|$ between the dominant contributions due to the terms $\propto m_1$ and $\propto m_2$.

5 Summary and Conclusions

We have presented here an $SU(5) \times T'$ unified model of flavour, which predicts the reactor neutrino mixing angle θ_{13} to be in the range determined by DayaBay [7] and RENO [8] experiments, and all other mixing angles are predicted to have values within the experimental uncertainties. It implements a type I seesaw mechanism and from the breaking of the discrete family symmetry T' we obtain tri-bimaximal mixing in the neutrino sector. The relatively large value of θ_{13} is then generated entirely by corrections coming from the charged lepton sector. This is a generic effect in GUTs where Yukawa couplings are related to each other. Here we have used recently proposed $SU(5)$ GUT relations [23] between the down-type quark Yukawa matrix and the charged lepton Yukawa matrix to get the relatively large prediction for the reactor mixing angle θ_{13} along the lines proposed in [16, 26].

The corrections to the solar and the atmospheric neutrino mixing angle are under control due to the structure of the charged lepton Yukawa matrix and the pattern of the complex CP violation phases. The model exhibits a special kind of CP violation, the so-called “geometrical” CP violation. All parameters and vevs are real and all non-trivial phases are coming from the complex Clebsch–Gordan coefficients of T' and are integer multiples of $\pi/4$. We have given the renormalisable superpotential which generates effectively the Yukawa matrices after integrating out heavy messenger fields and plugging in the family symmetry breaking flavon vevs. The flavon vevs point in special directions in flavour space and are all real. These results come out as solutions to the flavon alignment superpotential we have presented in the Appendix.

We have shown, in particular, that the phase pattern in the Yukawa matrices actually gives a very good fit of the quark and charged lepton masses and the CKM parameters at low energies. This fit fixes the charged lepton Yukawa matrix completely and since we find tri-bimaximal mixing in the neutrino sector itself, we can make predictions for the neutrino masses and all PMNS parameters. The angle θ_{13} is predicted to have a value corresponding to $\sin^2 \theta_{13} \cong 0.8 \sin^2 \theta^c / 2 = 0.02$. For the Dirac phase δ we obtain in the standard parametrisation of the PMNS matrix $\delta = 84.3^\circ$. Our model also predicts $\sin^2 \theta_{12} = 0.340$ and $\sin^2 \theta_{23} = 0.490$. There are three different possible solutions for the neutrino masses, two with normal ordering (NO, solutions A and B) and one with inverted ordering (IO). All three cases can be tested in experiments determining the absolute neutrino mass scale (or the sum of the three neutrino masses), in experiments which can measure the solar and atmospheric neutrino mixing angles with a high precision, in experiments searching for CP violation in neutrino oscillations and in neutrinoless double beta decay experiments. For the sum of three neutrino masses we get (with relatively small uncertainties, see Figs. (2) and (3)): $\sum_{k=1}^3 m_k = 6.31 \times 10^{-2}$ eV (NO, A); 6.54×10^{-2} eV (NO, B) and 12.1×10^{-2} eV (IO). The $(\beta\beta)_{0\nu}$ -decay effective Majorana mass for the three solutions is also unambiguously predicted: $|\langle m \rangle| = 4.90 \times 10^{-3}$ eV (NO, A); 7.95×10^{-3} eV (NO, B); 2.17×10^{-2} eV (IO). The three solutions differ only in the values of the three neutrino masses and of the Majorana phases, so that we make one single prediction for the rephasing invariant which determines the magnitude of CP violation effects in neutrino oscillations: $J_{\text{CP}} = 0.0324$. This value of J_{CP} is relatively large and can be tested in the experiments on CP violation in neutrino oscillations.

In conclusion, with the recent measurement of the last unknown neutrino mixing angle, neutrino physics has entered a new era. All angles are determined with a rather good precision, constraining flavour models severely. Since θ_{13} turned out to be relatively large, the observation of CP violation in the lepton sector might be feasible with data from the running and upcoming neutrino oscillation experiments. Explaining the data on leptonic CP violation would pose another challenge for flavour models. The model we proposed here is from this point of view rather comprehensive. Due to the GUT structure we can fit the quark masses and mixing parameters and the charged lepton masses, and using the latter we make definite predictions for the neutrino mass spectrum, the leptonic mixing angles and the leptonic CP violating phases. Our model is therefore testable in a variety of experiments. We are looking forward to the outcome of these tests.

Acknowledgements

This work was supported in part by the INFN program on “Astroparticle Physics”, by the Italian MIUR program on “Neutrinos, Dark Matter and Dark Energy in the Era of LHC” (A.M. and S.T.P.) and by the World Premier International Research Center Initiative (WPI Initiative), MEXT, Japan (S.T.P.). Furthermore the authors acknowledge partial support from the European Union under FP7 ITN INVISIBLES (Marie Curie Actions, PITN-GA-2011-289442).

A T' : The Rules of the Game

T' is the double-covering group of the tetrahedral symmetry T which is isomorphic to A_4 , the group of the even permutations of four objects. T' contains three inequivalent one-dimensional representations, called **1**, **1'** and **1''**, one three-dimensional, **3** and three two-dimensional repre-

$$\begin{aligned}
a \otimes \Gamma^p &= a\Gamma^p, \quad a \otimes a'(a'') = a'(a''), \quad a' \otimes a'(a'') = a''(a), \quad a'(a'') \otimes a'' = a(a') \\
\begin{pmatrix} x_1 \\ x_2 \end{pmatrix}_{\mathbf{2}} \otimes a'(a'') &= \begin{pmatrix} x_1 a'(a'') \\ x_2 a'(a'') \end{pmatrix}_{\mathbf{2}'(\mathbf{2}'')}, \quad \begin{pmatrix} y_1 \\ y_2 \end{pmatrix}_{\mathbf{2}'} \otimes a'(a'') = \begin{pmatrix} y_1 a'(a'') \\ y_2 a'(a'') \end{pmatrix}_{\mathbf{2}''(\mathbf{2})}, \quad \begin{pmatrix} z_1 \\ z_2 \end{pmatrix}_{\mathbf{2}''} \otimes a'(a'') = \begin{pmatrix} z_1 a'(a'') \\ z_2 a'(a'') \end{pmatrix}_{\mathbf{2}(\mathbf{2}')} \\
\begin{pmatrix} x_1 \\ x_2 \end{pmatrix}_{\mathbf{2}(\mathbf{2}')} \otimes \begin{pmatrix} x'_1 \\ x'_2 \end{pmatrix}_{\mathbf{2}(\mathbf{2}'')} &= \begin{pmatrix} x_1 x'_2 - x_2 x'_1 \\ \sqrt{2} \end{pmatrix}_{\mathbf{1}} \oplus \begin{pmatrix} \frac{(1-i)}{2}(x_1 x'_2 + x_2 x'_1) \\ i x_1 x'_1 \\ x_2 x'_2 \end{pmatrix}_{\mathbf{3}} \\
\begin{pmatrix} y_1 \\ y_2 \end{pmatrix}_{\mathbf{2}'(\mathbf{2})} \otimes \begin{pmatrix} y'_1 \\ y'_2 \end{pmatrix}_{\mathbf{2}'(\mathbf{2}'')} &= \begin{pmatrix} y_1 y'_2 - y_2 y'_1 \\ \sqrt{2} \end{pmatrix}_{\mathbf{1}''} \oplus \begin{pmatrix} i y_1 y'_1 \\ y_2 y'_2 \\ \frac{(1-i)}{2}(y_1 y'_2 + y_2 y'_1) \end{pmatrix}_{\mathbf{3}} \\
\begin{pmatrix} z_1 \\ z_2 \end{pmatrix}_{\mathbf{2}''(\mathbf{2})} \otimes \begin{pmatrix} z'_1 \\ z'_2 \end{pmatrix}_{\mathbf{2}''(\mathbf{2}')} &= \begin{pmatrix} z_1 z'_2 - z_2 z'_1 \\ \sqrt{2} \end{pmatrix}_{\mathbf{1}'} \oplus \begin{pmatrix} z_2 z'_2 \\ \frac{(1-i)}{2}(z_1 z'_2 + z_2 z'_1) \\ i z_1 z'_1 \end{pmatrix}_{\mathbf{3}} \\
(a')_{\mathbf{1}'} \otimes \begin{pmatrix} u_1 \\ u_2 \\ u_3 \end{pmatrix}_{\mathbf{3}} &= \begin{pmatrix} u_3 a' \\ u_1 a' \\ u_2 a' \end{pmatrix}_{\mathbf{3}}, \quad (a'')_{\mathbf{1}''} \otimes \begin{pmatrix} u_1 \\ u_2 \\ u_3 \end{pmatrix}_{\mathbf{3}} = \begin{pmatrix} u_2 a'' \\ u_3 a'' \\ u_1 a'' \end{pmatrix}_{\mathbf{3}} \\
\begin{pmatrix} x_1 \\ x_2 \end{pmatrix}_{\mathbf{2}} \otimes \begin{pmatrix} u_1 \\ u_2 \\ u_3 \end{pmatrix}_{\mathbf{3}} &= \frac{1}{\sqrt{3}} \left[\begin{pmatrix} (1+i)x_2 u_2 + x_1 u_1 \\ (1-i)x_1 u_3 - x_2 u_1 \end{pmatrix}_{\mathbf{2}} \oplus \begin{pmatrix} (1+i)x_2 u_3 + x_1 u_2 \\ (1-i)x_1 u_1 - x_2 u_2 \end{pmatrix}_{\mathbf{2}'} \oplus \begin{pmatrix} (1+i)x_2 u_1 + x_1 u_3 \\ (1-i)x_1 u_2 - x_2 u_3 \end{pmatrix}_{\mathbf{2}''} \right] \\
\begin{pmatrix} y_1 \\ y_2 \end{pmatrix}_{\mathbf{2}'} \otimes \begin{pmatrix} u_1 \\ u_2 \\ u_3 \end{pmatrix}_{\mathbf{3}} &= \frac{1}{\sqrt{3}} \left[\begin{pmatrix} (1+i)y_2 u_1 + y_1 u_3 \\ (1-i)y_1 u_2 - y_2 u_3 \end{pmatrix}_{\mathbf{2}} \oplus \begin{pmatrix} (1+i)y_2 u_2 + y_1 u_1 \\ (1-i)y_1 u_3 - y_2 u_1 \end{pmatrix}_{\mathbf{2}'} \oplus \begin{pmatrix} (1+i)y_2 u_3 + y_1 u_2 \\ (1-i)y_1 u_1 - y_2 u_2 \end{pmatrix}_{\mathbf{2}''} \right] \\
\begin{pmatrix} z_1 \\ z_2 \end{pmatrix}_{\mathbf{2}''} \otimes \begin{pmatrix} u_1 \\ u_2 \\ u_3 \end{pmatrix}_{\mathbf{3}} &= \frac{1}{\sqrt{3}} \left[\begin{pmatrix} (1+i)z_2 u_3 + z_1 u_2 \\ (1-i)z_1 u_1 - z_2 u_2 \end{pmatrix}_{\mathbf{2}} \oplus \begin{pmatrix} (1+i)z_2 u_1 + z_1 u_3 \\ (1-i)z_1 u_2 - z_2 u_3 \end{pmatrix}_{\mathbf{2}'} \oplus \begin{pmatrix} (1+i)z_2 u_2 + z_1 u_1 \\ (1-i)z_1 u_3 - z_2 u_1 \end{pmatrix}_{\mathbf{2}''} \right] \\
\begin{pmatrix} u_1 \\ u_2 \\ u_3 \end{pmatrix}_{\mathbf{3}} \otimes \begin{pmatrix} u'_1 \\ u'_2 \\ u'_3 \end{pmatrix}_{\mathbf{3}} &= \frac{1}{\sqrt{3}} [(u_1 u'_1 + u_2 u'_3 + u_3 u'_2)_{\mathbf{1}} \oplus (u_1 u'_2 + u_2 u'_1 + u_3 u'_3)_{\mathbf{1}'} \oplus (u_1 u'_3 + u_2 u'_2 + u_3 u'_1)_{\mathbf{1}''}] \oplus \\
&\quad \oplus \frac{1}{\sqrt{6}} \begin{pmatrix} 2u_1 u'_1 - u_2 u'_3 - u_3 u'_2 \\ 2u_3 u'_3 - u_1 u'_2 - u_2 u'_1 \\ 2u_2 u'_2 - u_1 u'_3 - u_3 u'_1 \end{pmatrix}_{\mathbf{3}} \oplus \frac{1}{\sqrt{2}} \begin{pmatrix} u_2 u'_3 - u_3 u'_2 \\ u_1 u'_2 - u_2 u'_1 \\ u_3 u'_1 - u_1 u'_3 \end{pmatrix}_{\mathbf{3}}
\end{aligned}$$

Table 7: The Clebsch–Gordan coefficients for the tensor products of T' .

Messenger Fields	$SU(5)$	T'	$U(1)_R$	Z_{12}^u	Z_8^d	Z_8^ν	Z_8	Z_6	Z'_6	Z_4
$\Sigma_1^a, \bar{\Sigma}_1^a$	1, 1	1, 1	0, 2	4, 8	0, 0	0, 0	0, 0	2, 4	2, 4	0, 0
$\Sigma_1^b, \bar{\Sigma}_1^b$	1, 1	1, 1	0, 2	4, 8	0, 0	0, 0	0, 0	0, 0	0, 0	0, 0
$\Sigma_{1'}^a, \bar{\Sigma}_{1'}^a$	1, 1	1', 1''	0, 2	6, 6	4, 4	4, 4	4, 4	0, 0	0, 0	2, 2
$\Sigma_{1'}^b, \bar{\Sigma}_{1'}^b$	1, 1	1', 1''	0, 2	8, 4	4, 4	4, 4	4, 4	4, 2	4, 2	0, 0
$\Sigma_{1'}^c, \bar{\Sigma}_{1'}^c$	1, 1	1', 1''	0, 2	8, 4	0, 0	0, 0	0, 0	2, 4	2, 4	0, 0
$\Sigma_{1''}^a, \bar{\Sigma}_{1''}^a$	1, 1	1'', 1'	0, 2	6, 6	4, 4	0, 0	4, 4	1, 5	1, 5	0, 0
$\Sigma_{1''}^b, \bar{\Sigma}_{1''}^b$	1, 1	1'', 1'	0, 2	0, 0	6, 2	2, 6	6, 2	3, 3	3, 3	0, 0
$\Sigma_{1''}^c, \bar{\Sigma}_{1''}^c$	24, 24	1'', 1'	0, 2	3, 9	2, 6	0, 0	6, 2	0, 0	3, 3	1, 3
$\Sigma_{2''}^a, \bar{\Sigma}_{2''}^a$	1, 1	2'', 2'	0, 2	9, 3	5, 3	7, 1	1, 7	3, 3	3, 3	3, 1
$\Sigma_{2''}^b, \bar{\Sigma}_{2''}^b$	1, 1	2'', 2'	0, 2	9, 3	4, 4	5, 3	3, 5	4, 2	1, 5	2, 2
$\Sigma_3^a, \bar{\Sigma}_3^a$	1, 1	3, 3	0, 2	6, 6	4, 4	0, 0	4, 4	1, 5	1, 5	0, 0
$\Sigma_3^b, \bar{\Sigma}_3^b$	1, 1	3, 3	0, 2	0, 0	6, 2	2, 6	6, 2	3, 3	3, 3	0, 0
$\Sigma_3^c, \bar{\Sigma}_3^c$	1, 1	3, 3	0, 2	0, 0	0, 0	4, 4	0, 0	3, 3	3, 3	2, 2
$\Sigma_3^d, \bar{\Sigma}_3^d$	1, 1	3, 3	0, 2	0, 0	0, 0	0, 0	4, 4	0, 0	3, 3	2, 2
$\Xi_{1'}^a, \bar{\Xi}_{1'}^a$	5, 5	1', 1''	1, 1	5, 7	0, 0	4, 4	0, 0	5, 1	5, 1	2, 2
$\Xi_{2'}^a, \bar{\Xi}_{2'}^a$	5, 5	2', 2''	1, 1	2, 10	7, 1	5, 3	3, 5	2, 4	5, 1	3, 1
$\Xi_{2''}^a, \bar{\Xi}_{2''}^a$	5, 5	2'', 2'	1, 1	8, 4	5, 3	7, 1	1, 7	2, 4	5, 1	1, 3
$\Omega_1^a, \bar{\Omega}_1^a$	5, 5	1, 1	0, 2	2, 10	0, 0	2, 10	4, 4	5, 1	5, 1	0, 0
$\Omega_{1'}^a, \bar{\Omega}_{1'}^a$	5, 5	1', 1''	2, 0	8, 4	0, 0	8, 4	0, 0	4, 2	4, 2	2, 2
$\Omega_{1'}^b, \bar{\Omega}_{1'}^b$	5, 5	1', 1''	2, 0	9, 3	1, 7	9, 3	2, 6	4, 2	1, 5	2, 2
$\Omega_{2''}^a, \bar{\Omega}_{2''}^a$	5, 5	2'', 2'	2, 0	9, 3	2, 6	9, 3	7, 1	1, 5	4, 2	2, 2
$\Omega_3^a, \bar{\Omega}_3^a$	5, 5	1, 1	0, 2	0, 0	3, 5	0, 0	4, 4	4, 2	4, 2	1, 3
$\Upsilon_{1''}^a, \bar{\Upsilon}_{1''}^a$	10, 10	1'', 1'	1, 1	2, 10	1, 7	5, 3	2, 6	3, 3	3, 3	2, 2
$\Upsilon_{1''}^b, \bar{\Upsilon}_{1''}^b$	10, 10	1'', 1'	1, 1	2, 10	0, 0	3, 5	4, 4	5, 1	2, 4	3, 1
$\Upsilon_2^a, \bar{\Upsilon}_2^a$	10, 10	2, 2	1, 1	11, 1	0, 0	2, 6	1, 7	4, 2	1, 5	3, 1
$\Upsilon_2^b, \bar{\Upsilon}_2^b$	10, 10	2, 2	1, 1	5, 7	2, 6	0, 0	7, 1	0, 0	0, 0	3, 1
$\Upsilon_2^c, \bar{\Upsilon}_2^c$	10, 10	2, 2	1, 1	5, 7	6, 2	4, 4	3, 5	0, 0	0, 0	3, 1
$\Upsilon_{2'}^a, \bar{\Upsilon}_{2'}^a$	10, 10	2', 2''	1, 1	11, 1	0, 0	2, 6	1, 7	4, 2	1, 5	3, 1
$\Upsilon_{2'}^b, \bar{\Upsilon}_{2'}^b$	10, 10	2', 2''	1, 1	5, 7	0, 0	4, 4	7, 1	4, 2	1, 5	3, 1
$\Upsilon_{2'}^c, \bar{\Upsilon}_{2'}^c$	10, 10	2', 2''	1, 1	5, 7	2, 6	0, 0	7, 1	0, 0	0, 0	3, 1
$\Upsilon_{2'}^d, \bar{\Upsilon}_{2'}^d$	10, 10	2', 2''	1, 1	11, 1	0, 0	2, 6	5, 3	2, 4	5, 1	3, 1
$\Upsilon_{2''}^a, \bar{\Upsilon}_{2''}^a$	10, 10	2'', 2'	1, 1	5, 7	4, 4	0, 0	7, 1	3, 3	0, 0	1, 3
$\Upsilon_{2''}^b, \bar{\Upsilon}_{2''}^b$	10, 10	2'', 2'	1, 1	11, 1	0, 0	2, 6	1, 7	4, 2	1, 5	3, 1
$\Upsilon_{2''}^c, \bar{\Upsilon}_{2''}^c$	10, 10	2'', 2'	1, 1	2, 10	2, 6	6, 2	7, 1	0, 0	3, 3	0, 0
$\Upsilon_{2''}^d, \bar{\Upsilon}_{2''}^d$	10, 10	2'', 2'	1, 1	11, 1	0, 0	2, 6	5, 3	2, 4	5, 1	3, 1
$\Upsilon_{2''}^e, \bar{\Upsilon}_{2''}^e$	10, 10	2'', 2'	1, 1	11, 1	0, 0	6, 2	5, 3	0, 0	0, 0	1, 3
$\Upsilon_3^a, \bar{\Upsilon}_3^a$	10, 10	3, 3	1, 1	2, 10	0, 0	7, 1	4, 4	4, 2	1, 5	1, 3
$\Upsilon_3^b, \bar{\Upsilon}_3^b$	10, 10	3, 3	1, 1	8, 4	0, 0	5, 3	2, 6	2, 4	5, 1	1, 3
$\Upsilon_3^c, \bar{\Upsilon}_3^c$	10, 10	3, 3	1, 1	8, 4	2, 6	5, 3	6, 2	5, 1	5, 1	3, 1
$\Upsilon_3^d, \bar{\Upsilon}_3^d$	10, 10	3, 3	1, 1	2, 10	5, 3	5, 3	6, 2	3, 3	0, 0	0, 0
$\Gamma_{2''}^a, \bar{\Gamma}_{2''}^a$	24, 24	2'', 2'	2, 0	9, 3	3, 5	5, 3	7, 1	3, 3	0, 0	1, 3

Table 8: Messenger fields used in our model. After integrating out these fields we end up with the desired effective operators. For the sake of brevity we do not list all mass terms in the text. The messenger pair in every line has a mass term and there are no cross terms allowed.

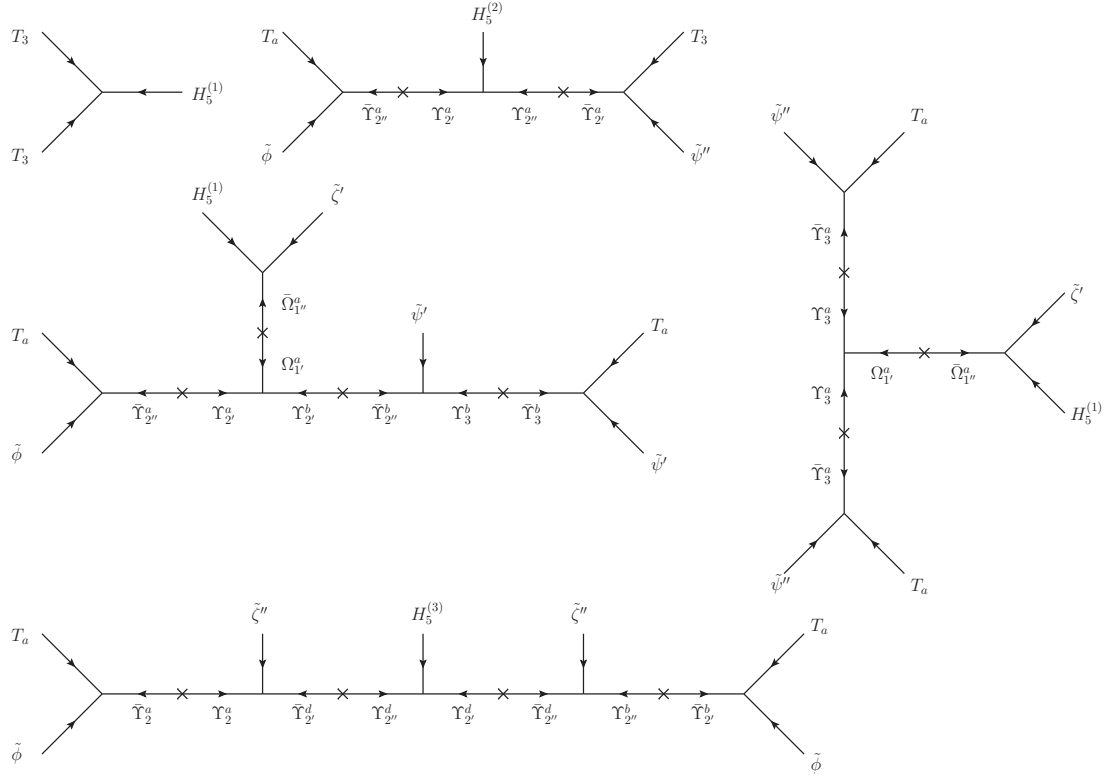


Figure 5: The supergraphs before integrating out the messengers for the up-type quark sector.

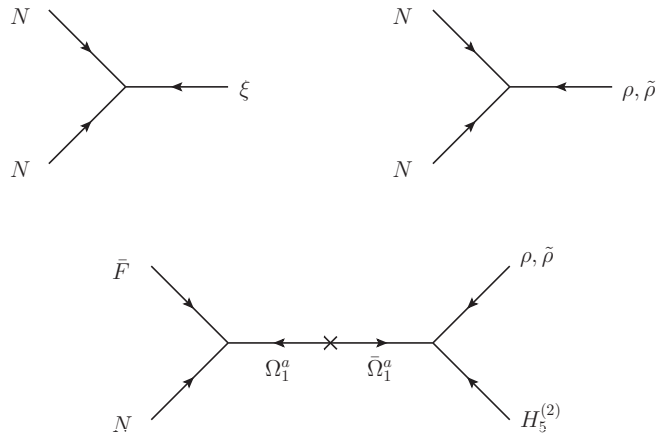


Figure 6: The supergraphs before integrating out the messengers for the neutrino sector.

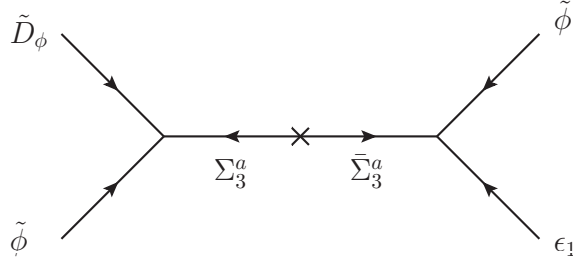


Figure 7: One typical diagram for the messengers in the flavon sector. We consider only effective operators up to dimension four. For the sake of brevity we only show one diagram. The other ones are quite similar with the driving field on one side and the auxiliary ϵ fields on the other side.

Apart from the messenger mass terms (which we do not write down explicitly) there are no terms with one or two fields involving matter, Higgs and flavon fields. For the down-type quark diagrams we find (here and in this whole section we do not write down the couplings)

$$\mathcal{W}_d^{\text{ren}} = \bar{F} \bar{H}_5^{(2)} \Upsilon_3^c + \phi \bar{\Upsilon}_3^c \Upsilon_{1''}^b + H_{24}'' T_3 \bar{\Upsilon}_1^b, \quad (\text{B.1})$$

$$+ T_a \phi \bar{\Upsilon}_{2''}^c + H_{24}'' \bar{\Upsilon}_2^c \Upsilon_{2'}^c + \psi' \Upsilon_2^c \bar{\Upsilon}_3^d + \bar{F} \bar{H}_5^{(1)} \Upsilon_3^d \quad (\text{B.2})$$

$$+ T_a \tilde{H}_{24}'' \bar{\Upsilon}_{2'}^c + \bar{H}_5^{(3)} \psi' \Omega_{2''}^a + \bar{\Omega}_2^a \psi' \Omega_3^a + \bar{\Omega}_3^a \Upsilon_{2''}^c \bar{\Xi}_{2''}^a, \quad (\text{B.3})$$

$$+ \bar{F} \psi' \Xi_{2'}^a + \bar{\Xi}_{2''}^a \Upsilon_{2''}^c \bar{\Omega}_{1''}^b + \zeta'' \bar{H}_5^{(1)} \Omega_{1'}^b + \zeta'' \bar{\Upsilon}_2^c \Upsilon_2^b + T_a \phi \bar{\Upsilon}_2^b \quad (\text{B.4})$$

$$+ \bar{F} \psi'' \Xi_{2''}^a + \bar{\Xi}_{2'}^a \Xi_{2''}^a \bar{\Gamma}_{2'}^a + H_{24}'' \psi'' \Gamma_{2''}^a + \bar{H}_5^{(3)} \bar{\Xi}_{1''}^a \Upsilon_{1''}^a + \bar{\Upsilon}_1^a T_a \psi'', \quad (\text{B.5})$$

for the up-type quarks

$$\mathcal{W}_u^{\text{ren}} = H_5^{(1)} T_3^2 + T_a \tilde{\phi} \bar{\Upsilon}_{2''}^a + H_5^{(2)} \Upsilon_{2'}^a \Upsilon_{2''}^a + T_3 \tilde{\psi}'' \bar{\Upsilon}_2^a, \quad (\text{B.6})$$

$$+ T_a \tilde{\psi}'' \bar{\Upsilon}_3^a + \zeta' H_5^{(1)} \bar{\Omega}_{1''}^a + \Omega_{1'}^a \Upsilon_3^a \Upsilon_3^a \quad (\text{B.7})$$

$$+ T_a \tilde{\phi} \bar{\Upsilon}_{2''}^a + \Upsilon_{2'}^a \Omega_{1'}^a \Upsilon_{2'}^b + H_5^{(1)} \zeta' \bar{\Omega}_{1''}^a + \tilde{\psi}' \bar{\Upsilon}_{2''}^b \Upsilon_3^b + \bar{\Upsilon}_3^b T_a \tilde{\psi}' \quad (\text{B.8})$$

$$+ T_a \tilde{\phi} \bar{\Upsilon}_2^a + \Upsilon_{2'}^a \tilde{\psi}'' \bar{\Upsilon}_{2'}^d + H_5^{(3)} \Upsilon_{2''}^d \Upsilon_{2''}^d + \zeta'' \bar{\Upsilon}_{2''}^d \Upsilon_{2''}^b + T_a \tilde{\phi} \bar{\Upsilon}_{2'}^b, \quad (\text{B.9})$$

and for the neutrino sector

$$\mathcal{W}_\nu^{\text{ren}} = N^2 \xi + N^2 \rho + N^2 \tilde{\rho} \bar{F} N \Omega_1^a + H_5^{(2)} \rho \bar{\Omega}_1^a + H_5^{(2)} \tilde{\rho} \bar{\Omega}_1^a. \quad (\text{B.10})$$

There are five additional operators which generate dimension eight or more operators in the matter sector, which we neglect. For completeness we give them as well

$$\mathcal{W}_{d \geq 8}^{\text{ren, matter}} = \zeta' \Upsilon_2^c \bar{\Upsilon}_{2''}^c + \bar{\Upsilon}_2^c \Upsilon_3^d \psi'' + \psi'' \Omega_{2''}^a \bar{\Omega}_3^a + \bar{\Gamma}_{2'}^a \bar{\Upsilon}_{2''}^c \Upsilon_3^d + \bar{\Gamma}_{2'}^a \bar{\Upsilon}_2^b \Upsilon_3^d. \quad (\text{B.11})$$

We turn now to the messengers, which give the non-renormalisable terms in the flavon alignment superpotential which we denote collectively with Σ . In this sector all the supergraphs have the structure as given in Fig. 7. (The role of the auxiliary ϵ fields is described in the next section and their quantum numbers are given in Tab. 10.) For the sake of brevity we do not give all the diagrams for the flavon sector, but all diagrams can easily be derived from the renormalisable flavon superpotential. We give here only the terms, where a messenger is

involved. The terms, where no messenger is involved will be discussed in the next section, when we discuss the superpotential responsible for the flavon alignment. The superpotential involving the Σ fields reads

$$\mathcal{W}_\Sigma^{\text{ren}} = D_\xi \xi \Sigma_3^c + D_\xi \rho \Sigma_3^c + D_\xi \tilde{\rho} \Sigma_3^c + \bar{\Sigma}_3^c \xi \epsilon_9 + \tilde{D}_\phi \tilde{\phi} \Sigma_3^a + \bar{\Sigma}_3^a \tilde{\phi} \epsilon_1 \quad (\text{B.12})$$

$$+ \tilde{D}_\phi \tilde{\phi} \Sigma_{1''}^a + \bar{\Sigma}_{1''}^a \tilde{\zeta}'' \epsilon_2 + D_\phi \phi \Sigma_3^b + \bar{\Sigma}_3^b \phi \epsilon_4 + D_\phi \phi \Sigma_{1''}^b + \bar{\Sigma}_{1''}^b \zeta'' \epsilon_5 \quad (\text{B.13})$$

$$+ D_\psi \psi'' \Sigma_{2''}^a + \bar{\Sigma}_{2''}^a \psi'' \epsilon_6 + D_\psi \phi \Sigma_{1'}^a + S_\zeta'' \epsilon_7 \Sigma_{1'}^a + \bar{\Sigma}_{1''}^a \zeta' \epsilon_7 + S_1 \psi' \Sigma_{2''}^b + \bar{\Sigma}_{2''}^b \psi'' \epsilon_8 \quad (\text{B.14})$$

$$+ S_2' \zeta' \Sigma_{1'}^b + \bar{\Sigma}_{1''}^b \zeta' \epsilon_{12} + S_2' \tilde{\zeta}' \Sigma_{1'}^c + \bar{\Sigma}_{1''}^c \tilde{\zeta}' \epsilon_{13} + S_{\epsilon_{12}} \epsilon_{12} \Sigma_1^a + \bar{\Sigma}_1^a \epsilon_{12}^2 \quad (\text{B.15})$$

$$+ S_{\epsilon_{13}} \epsilon_{13} \Sigma_1^b + \bar{\Sigma}_1^b \epsilon_{13}^2 + \tilde{S}_{24}'' \tilde{H}_{24}'' \Sigma_{1''}^c + \bar{\Sigma}_{1'}^c \epsilon_{10} \tilde{H}_{24}'' + \tilde{S}_{24}'' \xi \Sigma_3^d + \bar{\Sigma}_3^d \epsilon_{11} \xi . \quad (\text{B.16})$$

Apart from these there are as well operators which give dimension five operators in the flavon alignment superpotential after integrating out the messenger fields, which we will neglect. These operators are

$$\mathcal{W}_{d \geq 5}^{\text{ren, flavon}} = S_\zeta'' \Sigma_1^a \Sigma_{1'}^b + S_\zeta'' \Sigma_1^b \Sigma_{1'}^c + S_\zeta'' \Sigma_{1''}^a \Sigma_{1''}^a + S_\zeta'' \Sigma_{1''}^b \Sigma_{1''}^b + S_\zeta'' \Sigma_3^a \Sigma_3^a + S_\zeta'' \Sigma_3^b \Sigma_3^b \quad (\text{B.17})$$

$$+ S_{24}'' \Sigma_3^c \Sigma_3^c + S_{24}'' \Sigma_3^d \Sigma_3^d + (S_{\epsilon_i} + S_\xi + S_\rho) \Sigma_3^c \Sigma_3^c + (S_{\epsilon_i} + S_\xi + S_\rho) \Sigma_3^d \Sigma_3^d . \quad (\text{B.18})$$

Now we have discussed the messenger sector. After integrating out the messengers from the renormalisable superpotential we end up with the effective operators which give us the desired flavon vev alignments and structures of the Yukawa matrices.

C Flavon Vacuum Alignment

In this appendix we present the solution for our flavon vacuum alignment. In the present model all the discussed results crucially depend on the vev structure and on the fact that all flavon vevs are real.

In the flavon potential two new kinds of fields are introduced. First we have to add driving fields which are gauge singlets but transform in a non trivial way under the family and shaping symmetries and have a $U(1)_R$ charge of two. Minimising the F -term equations of this fields will give us the correct alignment (including phases) as one possible solution. Second we introduce auxiliary fields ϵ_i , $i = 1, \dots, 13$, which are singlets under $SU(5)$ and T' , but they transform in a non trivial way under the additional shaping symmetries. They appear only in the flavon superpotential. Indeed, these fields are introduced to compensate the charges of different operators, so that they are related to each other in the F -term equations. Note that we have to include for our alignment non-renormalisable operators, where we restrict ourselves to operators with mass dimension not higher than four in the superpotential. The driving fields are listed in Table 9 and the auxiliary fields are listed in Table 10.

Before going into the more complicated details of the flavon vacuum alignment we briefly discuss the “alignment” of the auxiliary flavons, which is simply the question how to give them a real vev. For this purpose we used the simple idea advocated in [38], which we can directly illustrate at the alignment for the ϵ fields itself. The superpotential for their alignment reads

$$\mathcal{W}_\epsilon = S_{\epsilon_i} (\epsilon_i^2 - M_{\epsilon_i}^2) + S_{\epsilon_j} \left(\frac{1}{\Lambda} \epsilon_j^3 - M_{\epsilon_j}^2 \right) , \quad (\text{C.1})$$

	\tilde{D}_ϕ	\tilde{S}_ψ	\tilde{S}''_ζ	\tilde{S}_ζ	D_ϕ	D_ψ	S''_ζ	D_ξ	S_ξ	S_ρ	S''_{24}	\tilde{S}''_{24}	S_1	S'_2	S_{ϵ_i}
T'	3	1	1''	1	3	3	1''	3	1	1	1''	1''	1	1'	1
Z_{12}^u	6	0	0	0	6	0	0	6	0	0	0	6	6	4	0
Z_8^d	4	0	0	0	0	2	4	4	0	0	0	4	5	0	0
Z_8^ν	4	0	0	0	4	2	4	4	0	0	0	0	2	0	0
Z_8	0	4	0	4	0	2	4	4	0	0	0	0	2	0	0
Z_6	1	0	4	0	3	0	0	3	0	0	0	0	5	2	0
Z'_6	1	0	4	0	0	3	0	3	0	0	0	3	5	2	0
Z_4	0	0	0	0	0	2	0	2	0	0	0	2	1	0	0

Table 9: List of the driving fields from the superpotential which give the desired vacuum alignment. All driving fields are $SU(5)$ gauge singlets and charged under $U(1)_R$ with charge +2.

	ϵ_1	ϵ_2	ϵ_3	ϵ_4	ϵ_5	ϵ_6	ϵ_7	ϵ_8	ϵ_9	ϵ_{10}	ϵ_{11}	ϵ_{12}	ϵ_{13}
Z_{12}^u	6	6	0	6	6	6	6	6	6	0	6	8	8
Z_8^d	4	4	0	4	0	4	0	4	4	0	0	0	4
Z_8^ν	4	0	0	0	4	0	0	4	4	0	0	0	0
Z_8	0	0	4	4	0	4	0	4	4	4	0	0	0
Z_6	3	3	0	3	3	0	0	0	3	0	0	4	0
Z'_6	3	3	0	3	3	0	0	0	3	0	0	4	0
Z_4	0	0	0	0	2	0	2	0	2	0	2	0	0

Table 10: List of the auxiliary flavon fields that do not couple to the matter sector. The ϵ_i fields are all $SU(5) \times T'$ singlets and carry no $U(1)_R$ charge.

where $i = 1, \dots, 11$ and $j = 12, 13$. Note that for the sake of readability we do not include any couplings. The driving fields S_{ϵ_i} and S_{ϵ_j} are total singlets so that terms like $S_{\epsilon} M_{\epsilon}^2$ are allowed. The F -Term equations for the driving fields give, e.g.

$$F_{S_{\epsilon_1}} = \epsilon_1^2 - M_{\epsilon_1}^2 = 0 . \quad (\text{C.2})$$

And since we assume that our fundamental theory is CP conserving the mass M_{ϵ_1} is real (like the coupling parameters which are not shown) and hence the vev of ϵ_1 is real and non-vanishing. For ϵ_{12} and ϵ_{13} this has to be slightly modified. For them we find three possible solutions, two of them complex and only one real. But we assume that the real solution is picked up, which could be preferred by higher order corrections, supergravity corrections or some low-energy soft terms in the scalar potential. To discuss these corrections in detail is beyond the scope of the current paper.

Note also that all the S_{ϵ_i} driving fields have the same quantum numbers and hence can mix with each other. In other words each of these driving fields could couple to each ϵ field. We have chosen here the basis in which the superpotential has the above structure, which makes the alignment clear (see also the appendix of [38]).

The same method can be applied to the real triplet and singlet flavons of our model, after we have fixed their alignment by some different kind of operators. But for the complex doublets ($\mathbf{2}', \mathbf{2}''$) and singlets ($\mathbf{1}', \mathbf{1}''$) we have to use other relations, because the representation squared cannot form a total singlet.

Before we come to this complex representations we discuss the alignment for the flavons appearing in the neutrino sector $(\xi, \rho, \tilde{\rho})$ where this complication is absent ⁴. The superpotential for these flavons reads

$$\mathcal{W}_{\xi, \rho, \tilde{\rho}} = \frac{D_{\xi}}{\Lambda} (\xi^2 \epsilon_9 + \xi \rho \epsilon_9 + \xi \tilde{\rho} \epsilon_9) + S_{\xi} (\xi^2 - M_{\xi}^2) + S_{\rho} (\rho^2 + \tilde{\rho}^2 - M_{\rho}^2) . \quad (\text{C.3})$$

The first thing to note here, is that we used the auxiliary flavon ϵ_9 in the first set of operators involving the triplet driving field D_{ξ} . Since ϵ_9 appears in all three operators, it drops out in the F -term conditions, but nevertheless it is real and hence would just modify the value of the vev without introducing any phase. The F -term conditions are

$$\frac{\partial \mathcal{W}_{\xi, \rho, \tilde{\rho}}}{\partial D_{\xi_1}} = 2\xi_1^2 - 2\xi_2 \xi_3 + \xi_1(\rho + \tilde{\rho}) = 0 , \quad (\text{C.4})$$

$$\frac{\partial \mathcal{W}_{\xi, \rho, \tilde{\rho}}}{\partial D_{\xi_2}} = 2\xi_2^2 - 2\xi_1 \xi_3 + \xi_2(\rho + \tilde{\rho}) = 0 , \quad (\text{C.5})$$

$$\frac{\partial \mathcal{W}_{\xi, \rho, \tilde{\rho}}}{\partial D_{\xi_3}} = 2\xi_3^2 - 2\xi_2 \xi_1 + \xi_3(\rho + \tilde{\rho}) = 0 , \quad (\text{C.6})$$

$$\frac{\partial \mathcal{W}_{\xi, \rho, \tilde{\rho}}}{\partial S_{\xi}} = \xi_1^2 + 2\xi_2 \xi_3 - M_{\xi}^2 = 0 , \quad (\text{C.7})$$

$$\frac{\partial \mathcal{W}_{\xi, \rho, \tilde{\rho}}}{\partial S_{\rho}} = \rho^2 + \tilde{\rho}^2 - M_{\rho}^2 = 0 . \quad (\text{C.8})$$

Besides the trivial solution $\xi_i = 0$, $i = 1, 2, 3$, we find for the first three of these equations by cyclic permutations in ξ_i the desired solution for which $\xi_i = \xi_0 \neq 0$ if $\rho_0 = -\tilde{\rho}_0$. The fact that

⁴ The alignment for the triplets follows the discussion in the seminal paper [39].

the vevs are non-vanishing and real can then be read off from the last two equations for which we used the method from [38] discussed above.

Now we come to the most complicated part of the flavon alignment sector, the flavons present in the quark and charged lepton sectors. Although we have two different set of flavons, one for the up-quark sector at the one hand and one for the down-type quark and charged lepton sector at the other hand, we cannot separate their alignments completely. In fact, we found that the alignment is itself independent from each other but the simplest solution which we found to make all vevs real involves cross couplings between the two sectors. The flavon superpotential reads

$$\mathcal{W}_f = \frac{\tilde{D}_\phi}{\Lambda} \left(\tilde{\phi}\tilde{\phi}\epsilon_1 + \tilde{\phi}\tilde{\zeta}''\epsilon_2 \right) + \tilde{S}_\zeta''(\tilde{\zeta}''\tilde{\zeta}'' + \tilde{\phi}\tilde{\phi} - M_{\tilde{\zeta}}\tilde{\zeta}') + \tilde{S}_\zeta(\tilde{\zeta}'\tilde{\zeta}'' - M_{\tilde{\zeta}}\epsilon_3) \quad (\text{C.9})$$

$$+ \tilde{S}_\psi \left(\tilde{\psi}'\tilde{\psi}'' - \tilde{\zeta}'\tilde{\zeta}'' \right) + \frac{D_\phi}{\Lambda} (\phi\phi\epsilon_4 + \phi\zeta''\epsilon_5) + \frac{D_\psi}{\Lambda} \left((\psi'')^2\epsilon_6 + \phi\zeta'\epsilon_7 \right) \quad (\text{C.10})$$

$$+ S_\psi (\psi'\psi'' - M_\psi^2) + S_\zeta'' \left(\zeta''\zeta'' + \phi\phi - M_{\zeta'}\zeta' + \frac{\epsilon_7^2}{\Lambda}\zeta' \right) \quad (\text{C.11})$$

$$+ S_1 \left(\psi'\tilde{\psi}''\frac{\epsilon_8}{\Lambda} - M_{S_1}^2 \right) + S_2' \left((\zeta')^2\epsilon_{12} - (\tilde{\zeta}')^2\epsilon_{13} \right), \quad (\text{C.12})$$

where in the last equations the cross couplings between the two sectors are written. We do not want to discuss here all the details of the alignment in detail, instead we will only discuss the phases of the vevs of the complex fields in a bit more detail. Nevertheless, we quote all the F -term conditions, in which it is then quite easy to plug in the flavon vevs from eqs. (2.1)-(2.3) and see that they form a viable solution. The F -term conditions read for the up sector

$$\frac{\partial \mathcal{W}_f}{\partial \tilde{D}_{\phi_1}} = \epsilon_1(2\tilde{\phi}_1^2 - 2\tilde{\phi}_2\tilde{\phi}_3) + \epsilon_2\tilde{\phi}_2\tilde{\zeta}'' = 0, \quad (\text{C.13})$$

$$\frac{\partial \mathcal{W}_f}{\partial \tilde{D}_{\phi_2}} = \epsilon_1(2\tilde{\phi}_2^2 - 2\tilde{\phi}_1\tilde{\phi}_3) + \epsilon_2\tilde{\phi}_1\tilde{\zeta}'' = 0, \quad (\text{C.14})$$

$$\frac{\partial \mathcal{W}_f}{\partial \tilde{D}_{\phi_3}} = \epsilon_1(2\tilde{\phi}_3^2 - 2\tilde{\phi}_1\tilde{\phi}_2) + \epsilon_2\tilde{\phi}_3\tilde{\zeta}'' = 0, \quad (\text{C.15})$$

$$\frac{\partial \mathcal{W}_f}{\partial \tilde{S}_\zeta''} = (\tilde{\zeta}'')^2 - M_{\tilde{\zeta}}\tilde{\zeta}' + \tilde{\phi}_3^2 + 2\tilde{\phi}_1\tilde{\phi}_2 = 0, \quad (\text{C.16})$$

$$\frac{\partial \mathcal{W}_f}{\partial \tilde{S}_\zeta} = \tilde{\zeta}'\tilde{\zeta}'' - M_{\tilde{\zeta}}\epsilon_3 = 0, \quad (\text{C.17})$$

$$\frac{\partial \mathcal{W}_f}{\partial \tilde{S}_\psi} = \tilde{\psi}_1'\tilde{\psi}_2'' - \tilde{\psi}_2'\tilde{\psi}_1'' - \tilde{\zeta}'\tilde{\zeta}'' = 0, \quad (\text{C.18})$$

for the down sector

$$\frac{\partial \mathcal{W}_f}{\partial D_{\phi_1}} = \epsilon_4(2\phi_1^2 - 2\phi_2\phi_3) + \epsilon_5\phi_2\zeta'' = 0, \quad (\text{C.19})$$

$$\frac{\partial \mathcal{W}_f}{\partial D_{\phi_2}} = \epsilon_4(2\phi_2^2 - 2\phi_1\phi_3) + \epsilon_5\phi_1\zeta'' = 0, \quad (\text{C.20})$$

$$\frac{\partial \mathcal{W}_f}{\partial D_{\phi_3}} = \epsilon_4(2\phi_3^2 - 2\phi_1\phi_2) + \epsilon_5\phi_3\zeta'' = 0, \quad (\text{C.21})$$

$$\frac{\partial \mathcal{W}_f}{\partial D_{\psi_1}} = \epsilon_6((\psi_2'')^2) + \epsilon_7\phi_3\zeta' = 0, \quad (\text{C.22})$$

$$\frac{\partial \mathcal{W}_f}{\partial D_{\psi_2}} = i \epsilon_6 ((\psi_1'')^2 + \epsilon_7 \phi_2 \zeta') = 0 , \quad (\text{C.23})$$

$$\frac{\partial \mathcal{W}_f}{\partial D_{\psi_3}} = (1 - i) \epsilon_6 \psi_1'' \psi_2'' + \epsilon_7 \phi_1 \zeta' = 0 , \quad (\text{C.24})$$

$$\frac{\partial \mathcal{W}_f}{\partial S_\psi} = \psi_1' \psi_2'' - \psi_2' \psi_1'' - M_\psi^2 = 0 , \quad (\text{C.25})$$

$$\frac{\partial \mathcal{W}_f}{\partial S_\zeta''} = (\zeta'')^2 - \left(M_{\zeta'} + \frac{\epsilon_7^2}{\Lambda} \right) \zeta' = 0 , \quad (\text{C.26})$$

and for the cross couplings between the two sectors

$$\frac{\partial \mathcal{W}_f}{\partial S_1} = \left(\psi_1' \tilde{\psi}_2'' - \psi_2' \tilde{\psi}_1'' \right) \frac{\epsilon_8}{\Lambda} - M_{S_1}^2 = 0 , \quad (\text{C.27})$$

$$\frac{\partial \mathcal{W}_f}{\partial S_2'} = (\zeta')^2 \epsilon_{12} - (\tilde{\zeta}')^2 \epsilon_{13} = 0 . \quad (\text{C.28})$$

So how do we make the vevs of the complex representations real? Exemplary we discuss the complex singlets $\tilde{\zeta}''$, $\tilde{\zeta}'$, ζ'' and ζ' . From eqs. (C.16) and (C.17) we find a polynomial in $\tilde{\zeta}''$

$$(\tilde{\zeta}'')^3 + \tilde{\zeta}''(\tilde{\phi}_3^2 + 2\tilde{\phi}_1\tilde{\phi}_2) - M_{\tilde{\zeta}'} M_{\tilde{\zeta}} \epsilon_3 = 0 , \quad (\text{C.29})$$

which has a real solution (at least for a certain choice of parameters and plugging in the real vev of $\tilde{\phi}$) which we pick here. Then we know that $(\tilde{\zeta}'')^3$ is real, while $\tilde{\zeta}'$ has the opposite phase of $\tilde{\zeta}''$ so it is real as well. From eq. (C.28) we then find ζ' to be real and from eq. (C.26) we obtain ζ'' to be real and all the singlet vevs are real. For the doublets a similar mechanism applies.

The last alignment we want to discuss here is strictly speaking not an alignment. But since we have used adjoints of $SU(5)$ in our operators to get the desired Yukawa coupling relations between the charged leptons and the down-type quarks we add here a mechanism which generates the vev of these adjoints and also show explicitly that they are real. For the fields H_{24}'' and \tilde{H}_{24}'' we can write down the following superpotential using the two driving fields S_{24}'' and \tilde{S}_{24}''

$$\mathcal{W}_{24} = S_{24}'' (H_{24}'' H_{24}'' - \xi^2) + \frac{\tilde{S}_{24}''}{\Lambda} \left(\tilde{H}_{24}'' \tilde{H}_{24}'' \epsilon_{10} - \xi^2 \epsilon_{11} \right) . \quad (\text{C.30})$$

We see that the vev of ξ triggers a vev for the two adjoint fields and even more these two vevs are directly related to the T' symmetry breaking scale. That means that in our model the GUT scale and the scale of T' coincide (up to some order one coefficients). In principle, we can again choose here between two different vevs for the adjoints. One pointing into the SM direction and the other one pointing into the $SU(4) \times U(1)$ direction and we assume the first option to be realised. We also note here, that the solution of the Doublet-Triplet-Splitting problem and hence the construction of the whole Higgs sector is clearly beyond the scope of this paper.

References

- [1] K. Nakamura *et al.* (Particle Data Group), J. Phys. **G 37** (2010) 075021.
- [2] S.M. Bilenky, J. Hosek and S.T. Petcov, Phys. Lett. B **94** (1980) 495.
- [3] K. Abe *et al.* [T2K Collaboration], Phy. Rev. Lett. **107** (2011) 041801 [arXiv:1106.2822].

- [4] P. Adamson *et al.* [MINOS Collaboration], *Phys. Rev. Lett.* **107** (2011) 181802.
- [5] Y. Abe *et al.* [Double Chooz Collaboration], arXiv:1112.6353.
- [6] G. L. Fogli, E. Lisi, A. Marrone, A. Palazzo and A. M. Rotunno, *Phys. Rev. D* **84** (2011) 053007 [arXiv:1106.6028 [hep-ph]].
- [7] F. P. An *et al.* [DAYA-BAY Collaboration], arXiv:1203.1669 [hep-ex].
- [8] J.K. Ahn *et al.* [RENO Collaboration], arXiv:1204.0626.
- [9] M. Mezzetto and T. Schwetz, *J. Phys. G* **37** (2010) 103001 [arXiv:1003.5800].
- [10] M. Tortola, J. W. F. Valle and D. Vanegas, arXiv:1205.4018 [hep-ph].
- [11] G. Mention *et al.*, *Phys. Rev. D* **83** (2011) 073008.
- [12] P. Minkowski, *Phys. Lett. B* **67** (1977) 421; M. Gell-Mann, P. Ramond and R. Slansky in Sanibel Talk, CALT-68-709, Feb 1979, and in *Supergravity* (North Holland, Amsterdam 1979); T. Yanagida in *Proc. of the Workshop on Unified Theory and Baryon Number of the Universe*, KEK, Japan, 1979; S.L.Glashow, Cargese Lectures (1979); R. N. Mohapatra and G. Senjanovic, *Phys. Rev. Lett.* **44** (1980) 912.
- [13] P. F. Harrison, D. H. Perkins and W. G. Scott, *Phys. Lett. B* **530**, 167 (2002); *Phys. Lett. B* **535**, 163 (2002); Z. Z. Xing, *Phys. Lett. B* **533**, 85 (2002); X. G. He and A. Zee, *Phys. Lett. B* **560**, 87 (2003); see also L. Wolfenstein, *Phys. Rev. D* **18**, 958 (1978).
- [14] P.H. Frampton, S.T. Petcov and W. Rodejohann, *Nucl. Phys. B* **687**, 31 (2004); A. Romanino, *Phys. Rev. D* **70**, 013003 (2004).
- [15] K.A. Hochmuth, S.T. Petcov and W. Rodejohann, *Phys. Lett B* **654** (2007) 177.
- [16] D. Marzocca, S. T. Petcov, A. Romanino and M. Spinrath, *JHEP* **1111** (2011) 009 [arXiv:1108.0614 [hep-ph]].
- [17] F. Feruglio, C. Hagedorn, Y. Lin and L. Merlo, *Nucl. Phys. B* **775** (2007) 120 [Erratum-ibid. **836** (2010) 127] [hep-ph/0702194].
- [18] P. H. Frampton and T. W. Kephart, *Int. J. Mod. Phys. A* **10** (1995) 4689 [hep-ph/9409330]; P. H. Frampton, T. W. Kephart and S. Matsuzaki, *Phys. Rev. D* **78** (2008) 073004 [arXiv:0807.4713 [hep-ph]]; D. A. Eby, P. H. Frampton and S. Matsuzaki, *Phys. Lett. B* **671** (2009) 386 [arXiv:0810.4899 [hep-ph]]; P. H. Frampton and S. Matsuzaki, *Phys. Lett. B* **679** (2009) 347 [arXiv:0902.1140 [hep-ph]].
- [19] J.-Q. Chen and P.-D. Fan, *J. Math. Phys.* **39**, 5519 (1998).
- [20] M.-C. Chen and K. T. Mahanthappa, *Phys. Lett. B* **681**, 444 (2009);
- [21] M.-C. Chen and K. T. Mahanthappa, *Phys. Lett. B* **652**, 34 (2007);
- [22] M. -C. Chen, K. T. Mahanthappa, A. Meroni and S. T. Petcov, arXiv:1109.0731 [hep-ph].
- [23] S. Antusch and M. Spinrath, *Phys. Rev. D* **79** (2009) 095004 [arXiv:0902.4644 [hep-ph]]; M. Spinrath, arXiv:1009.2511 [hep-ph].

- [24] S. Antusch, S. F. King, M. Malinsky and M. Spinrath, Phys. Rev. D **81** (2010) 033008 [arXiv:0910.5127 [hep-ph]].
- [25] H. Georgi and C. Jarlskog, Phys. Lett. B **86** (1979) 297.
- [26] S. Antusch and V. Maurer, Phys. Rev. D **84** (2011) 117301 [arXiv:1107.3728 [hep-ph]].
- [27] L. J. Hall, R. Rattazzi and U. Sarid, Phys. Rev. D **50** (1994) 7048 [arXiv:hep-ph/9306309]; M. S. Carena, M. Olechowski, S. Pokorski and C. E. M. Wagner, Nucl. Phys. B **426** (1994) 269 [arXiv:hep-ph/9402253]; R. Hempfling, Phys. Rev. D **49** (1994) 6168; T. Blazek, S. Raby and S. Pokorski, Phys. Rev. D **52** (1995) 4151 [arXiv:hep-ph/9504364].
- [28] S. Antusch and M. Spinrath, Phys. Rev. D **78** (2008) 075020 [arXiv:0804.0717 [hep-ph]].
- [29] S. Antusch, L. Calibbi, V. Maurer and M. Spinrath, Nucl. Phys. B **852** (2011) 108 [arXiv:1104.3040 [hep-ph]].
- [30] S. Antusch, J. Kersten, M. Lindner, M. Ratz and M. A. Schmidt, JHEP **0503** (2005) 024 [hep-ph/0501272].
- [31] Z.-z. Xing, H. Zhang, S. Zhou, Phys. Rev. **D77** (2008) 113016. [arXiv:0712.1419 [hep-ph]].
- [32] H. Leutwyler, Nucl. Phys. Proc. Suppl. **94** (2001) 108-115. [hep-ph/0011049].
- [33] CKMfitter Group (J. Charles et al.), Eur. Phys. J. C **41** (2005) 1, hep-ph/0406184, updated results and plots: <http://ckmfitter.in2p3.fr>; M. Bona et al. (UTfit Collaboration), hep-ph/0701204.
- [34] C. Hagedorn, E. Molinaro, S.T. Petcov, JHEP **09** (2009) 115.
- [35] C. Jarlskog, Z. Phys. C **29** 491 (1985); Phys. Rev. Lett. **55**, 1039 (1985).
- [36] P.I. Krastev and S. T. Petcov, Phys. Lett. B **205**, 84 (1988).
- [37] S. M. Bilenky and S. T. Petcov, Rev. Mod. Phys. **59** (1987) 671; S.M. Bilenky, S. Pascoli and S.T. Petcov, Phys. Rev. D **64** (2001) 053010; S. Pascoli and S.T. Petcov, Phys. Rev. **D77** (2008) 113003; W. Rodejohann, Int. J. Mod. Phys. E **20** (2011) 1833.
- [38] S. Antusch, S. F. King, C. Luhn and M. Spinrath, Nucl. Phys. B **850** (2011) 477 [arXiv:1103.5930 [hep-ph]].
- [39] G. Altarelli and F. Feruglio, Nucl. Phys. B **741** (2006) 215 [hep-ph/0512103].